ELEMENTA
Science of the Anthropocene

Gérikas Ribeiro, C, et al. 2020. Culturable diversity of Arctic phytoplankton during pack ice melting. *Elem Sci Anth,* 8: 6. DOI: https://doi.org/10.1525/elementa.401

RESEARCH ARTICLE

Culturable diversity of Arctic phytoplankton during pack ice melting

Catherine Gérikas Ribeiro[*,†], Adriana Lopes dos Santos[†,‡], Priscillia Gourvil[§], Florence Le Gall[*], Dominique Marie[*], Margot Tragin[*], Ian Probert[§] and Daniel Vaulot[*,‡]

Massive phytoplankton blooms develop at the Arctic ice edge, sometimes extending far under the pack ice. An extensive culturing effort was conducted before and during a phytoplankton bloom in Baffin Bay between April and July 2016. Different isolation strategies were applied, including flow cytometry cell sorting, manual single cell pipetting, and serial dilution. Although all three techniques yielded the most common organisms, each technique retrieved specific taxa, highlighting the importance of using several methods to maximize the number and diversity of isolated strains. More than 1,000 cultures were obtained, characterized by 18S rRNA sequencing and optical microscopy, and de-replicated to a subset of 276 strains presented in this work. Strains grouped into 57 phylotypes defined by 100% 18S rRNA sequence similarity. These phylotypes spread across five divisions: Heterokontophyta, Chlorophyta, Cryptophyta, Haptophyta and Dinophyta. Diatoms were the most abundant group (193 strains), mostly represented by the genera *Chaetoceros* and *Attheya*. The genera *Baffinella* and *Pyramimonas* were the most abundant non-diatom nanoplankton strains, while *Micromonas polaris* dominated the picoplankton. Diversity at the class level was higher during the peak of the bloom. Potentially new species were isolated, in particular within the genera *Navicula*, *Nitzschia*, *Coscinodiscus*, *Thalassiosira*, *Pyramimonas*, *Mantoniella* and *Isochrysis*. Culturing efforts such as this one highlight the unexplored eukaryotic plankton diversity in the Arctic and provide a large number of strains for analyzing physiological and metabolic impacts in this changing environment.

Keywords: Arctic diatoms; Arctic flagellates; Isolation techniques; 18S rRNA; Roscoff culture collection; Sympagic phytoplankton communities

Introduction

Polar algal communities impact (Lutz et al., 2016) and are impacted by (Brown and Arrigo, 2013) ice melting cycles. The tight links between phytoplankton diversity/production and sea ice dynamics are beginning to be decoded and seem to be fairly complex (Arrigo et al., 2014; Olsen et al., 2017). Due to increased light availability and vertical mixing, the shrinking of pack ice and the shift from thick multi-year ice to thinner first-year ice has been linked to enhanced Arctic primary production (Arrigo et al., 2008; Brown and Arrigo, 2013). However, the salinity decrease in surface waters, resulting from higher ice melting rates and increased river run off, leads to an increase in water column stratification which in turn may impact nutrient availability and plankton diversity (Li et al., 2009). The presence of ice-associated algae may impact the quantity (Leu et al., 2011; Kohlbach et al., 2016) and quality (Duerksen et al., 2014; Schmidt et al., 2018) of secondary production at high latitudes, as well as the recruitment of ice-associated diatoms to the water column (Kauko et al., 2018). Climate-related changes can also increase Arctic vulnerability to invasive species (Vincent, 2010) as the intrusion of warmer waters "atlantifies" the Arctic Ocean (Årthun et al., 2012) and temperate phytoplankton move northwards, replacing Arctic communities (Neukermans et al., 2018).

Massive Arctic phytoplankton blooms have been detected not only along the ice edge (Perrette et al., 2011), but also extending large distances under the pack ice (Arrigo et al., 2012). The increasingly thin pack ice and the formation of melt ponds may favor areas experiencing sub-ice bloom formation that may reach almost one third of the ice-covered Arctic Ocean in the summer (Horvat et al., 2017).

The Arctic phytoplankton community exhibits strong seasonal variability (Sherr et al., 2003), with smaller organisms (picoplankton) dominating during winter and early

* Sorbonne Université, CNRS, UMR7144, Team ECOMAP, Station Biologique de Roscoff, Roscoff, FR

† GEMA Center for Genomics, Ecology and Environment, Universidad Mayor, Santiago, CL

‡ Nanyang Technological University, Asian School of the Environment, SG

§ Sorbonne Université, CNRS, FR2424, Roscoff Culture Collection, Station Biologique de Roscoff, Roscoff, FR

Corresponding author: Catherine Gérikas Ribeiro (catherine.gerikas@gmail.com)

summer, followed by diatoms during the spring bloom (Marquardt et al., 2016). The green alga *Micromonas* (Mamiellophyceae) is recognized as the dominant pico-phytoplankton (0.2–3.0 μm) genus during the Arctic summer (Lovejoy et al., 2007; Balzano et al., 2017). The genus *Micromonas* is widespread throughout the world oceans (Worden et al., 2009; Tragin and Vaulot, 2019) and genetically diversified (Simon et al., 2017) in relation to thermal niches (Demory et al., 2018), with one species, *Micromonas polaris*, restricted to polar regions. Another species of Mamiellophyceae, *Bathycoccus prasinos*, may replace *M. polaris* during polar winter (Joli et al., 2017).

Regarding the more diverse Arctic nano-phytoplankton, the genus *Pyramimonas* has often been reported (Lovejoy et al., 2002; Joli et al., 2017) displaying high intra-generic diversity (Daugbjerg and Moestrup, 1993; Balzano et al., 2012) and associated with sea ice (Harðardóttir et al., 2014; Kauko et al., 2018). The mamiellophyte *Mantoniella* is reported to a lesser extent in Arctic waters (Lovejoy et al., 2007; Terrado et al., 2013; Joli et al., 2017), although diversity within this genus seems to be higher than other polar Mamiellophyceae (Yau et al., 2019). Other commonly observed Arctic taxa include the bloom-forming genus *Phaeocystis* (Assmy et al., 2017), unidentified Pelagophyceae, the mixotrophic and cosmopolitan *Dinobryon faculiferum*, and the genus *Chlamydomonas* (Lovejoy et al., 2002; Balzano et al., 2012; Terrado et al., 2013; Crawford et al., 2018).

Large size classes of polar phytoplankton are dominated by diatoms and dinoflagellates (Crawford et al., 2018). Diatoms constitute a large fraction of polar phytoplankton communities, especially in coastal areas and during episodic upwelling (Sherr et al., 2003; Arrigo et al., 2014), impacting carbon flux to the benthic community (Booth et al., 2002). This group is particularly important during late spring/summer months in the pelagic environment (Lovejoy et al., 2002; Balzano et al., 2012), but also comprises a significant portion of protist biomass during young ice formation (Kauko et al., 2018) and of taxa diversity in first-year ice during the dark Arctic winter (Niemi et al., 2011). Successional patterns in diatom diversity are observed during Arctic spring bloom development, possibly linked with temperature optima or transportation from lower latitudes (Quillfeldt, 2000). The genera most often reported among Arctic centric diatoms are *Chaetoceros* and *Thalassiosira* (Lovejoy et al., 2002; Johnsen et al., 2018). *Chaetoceros gelidus* and *Chaetoceros neogracilis* often dominate Arctic phytoplankton assemblages (Katsuki et al., 2009; Crawford et al., 2018), although other species such as *Chaetoceros decipiens* or *Chaetoceros furcellatus* have also been reported (Joo et al., 2012; Johnsen et al., 2018). *Thalassiosira* is a diverse genus with both Arctic, ice-associated and subpolar/temperate water representatives (Luddington et al., 2016), in particular *Thalassiosira nordenskioeldii* and *Thalassiosira antarctica* var. *borealis* (Quillfeldt, 2000; Lovejoy et al., 2002; Johnsen et al., 2018). High abundances of pennate diatoms are linked to late autumn/winter sea ice (Niemi et al., 2011) and bottom communities (Kauko et al., 2018; Leeuwe et al., 2018). The most commonly reported genera include *Cylindrotheca*, *Fragilariopsis*, *Navicula*, *Nitzschia* and *Pseudo-nitzschia* (Katsuki et al., 2009; Poulin et al., 2011; Leeuwe et al., 2018). In contrast to diatoms and small flagellates that present a strong seasonal signal, dinoflagellates are prevalent throughout the year (Comeau et al., 2011; Marquardt et al., 2016), although some taxa vary seasonally (Onda et al., 2017).

Culturing efforts in the Arctic have been scarce, with one campaign in early spring in northern Baffin Bay in 1998 (Potvin and Lovejoy, 2009) and the MALINA cruise in summer 2009, which covered the Northeast Pacific Ocean, the Bering Strait, the Chukchi and Beaufort Seas (Balzano et al., 2012, 2017). As microbial communities respond to the rapid loss in Arctic ice cover and thickness (Vincent, 2010; Comeau et al., 2011), efforts to culture phytoplankton from the region are important in order to have at our disposal reference strains whose physiology and taxonomy can be studied in the laboratory under controlled conditions. In the present work, Baffin Bay samples from both an ice camp at a fixed station and an icebreaker cruise were obtained for phytoplankton isolation before, during and at the peak of the Arctic spring bloom. More than 1,000 cultures were obtained by serial dilution, single cell pipetting and flow cytometry (FCM) cell sorting, characterized by partial 18S rRNA sequencing and optical microscopy and de-replicated to a subset of 276 strains presented here.

Materials and Methods

Sampling

The Green Edge project (http://www.greenedgeproject.info) aimed at investigating the dynamics of the Arctic spring bloom at the ice edge. Samples for phytoplankton isolation were obtained both at a fixed station (Ice Camp) and during a cruise onboard the Canadian icebreaker CCGS *Amundsen*.

The ice camp (IC) was set up near the Inuit village of Qikiqtarjuaq, Nunavut, on Baffin Island (67° 28' N, 63° 47' W), in a location identified to have little influence from continental drainage (**Figure 1**). To observe the changes in the phytoplankton community during the ice melting process, sampling was carried out between 4 May and 18 July 2016. Samples were collected in the water column under the ice at two depths three times a week and from melted ice cores once per week. The ice cores were melted at room temperature with the addition of 0.2 μm filtered sea water prior to isolation procedures.

The *Amundsen* cruise (AM) took place between 3 June and 14 July 2016 in Baffin Bay, Canada, between 60°N and 70°N. (**Figure 1**). Sampling transects were designed to cross the marginal ice zone perpendicularly in order to observe changes in the phytoplankton community from open water to solid sea ice (**Figure 1**). Seawater for isolation was sampled approximately every two days at two depths with Niskin bottles mounted on a CTD frame Sea-Bird SBE-911 plus.

The development of the spring phytoplankton bloom at the IC site was monitored by flow cytometry (Massicotte et al., 2020), and its phases were defined as follows: 'pre-bloom' from 4 May to 23 May; 'bloom-development' from 24 May to 22 June and 'bloom-peak' from 23 June to

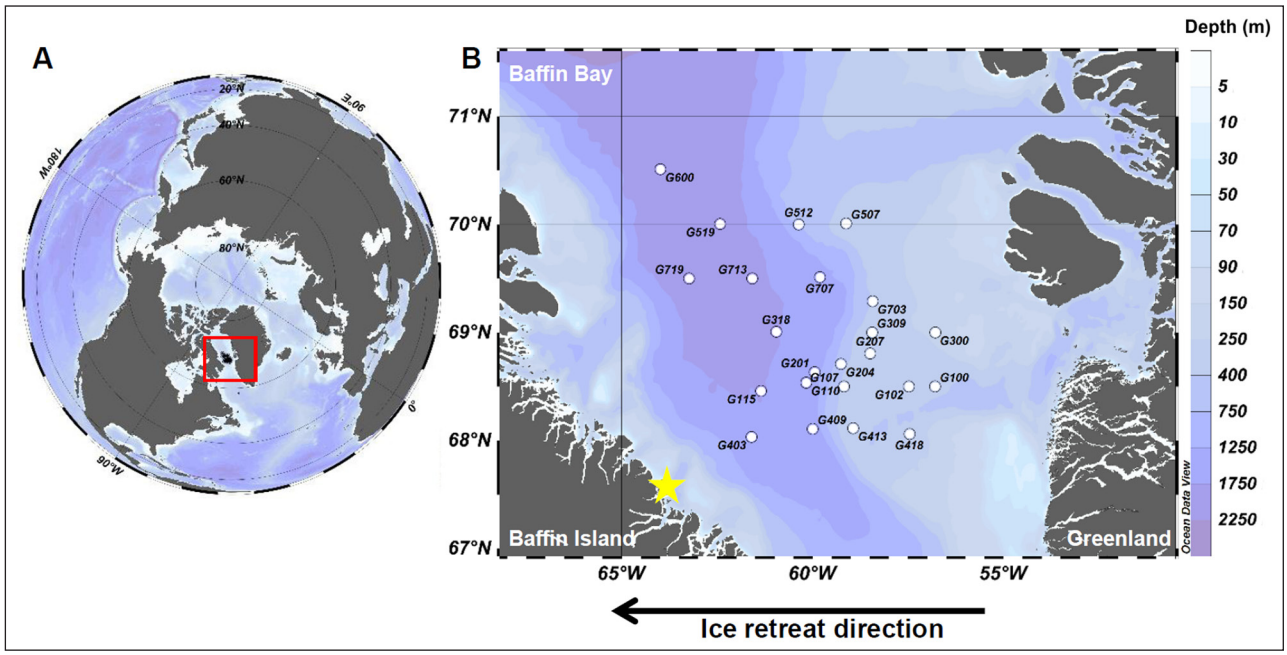

Figure 1: Sampling stations. Sampling stations where phytoplankton strains were retrieved. **A)** Sampling region (red square). **B)** The yellow star indicates the location of the Green Edge Ice Camp (IC) (67.48°N, 63.79°W); *Amundsen* cruise (AM) stations are marked by white dots; black arrow indicates the ice retreat direction during the melting process; color scale indicates depth contours in meters. DOI: https://doi.org/10.1525/elementa.401.f1

18 July. AM strains were not related to bloom phases due to spatial variability across the marginal ice zone during sampling.

Strain isolation and maintenance

Several isolation strategies were employed in order to maximize the number and diversity of cultures retrieved. Different pre-isolation procedures were applied to different samples, which included filtration, concentration and enrichment. In order to target the smaller plankton size fractions, samples were gravity pre-filtered with 3 μm and 0.8 μm filters prior to enrichment or serial dilution, as described previously (Le Gall et al., 2008; Balzano et al., 2017). Some samples were concentrated with tangential flow filtration (Vivaflow Cartridge 200, Sartorius) with a 0.2 μm polyethersulfone membrane using 2 L of seawater or 0.5 L of ice core melted into filtered seawater (roughly 1 volume of ice for 5 volumes of sea water). Enrichment was performed by mixing 25 mL of pre-filtered seawater with 1 mL of L1 (Guillard and Hargraves, 1993) or PCR-S11 culture medium (Rippka et al., 2000) (media recipes at http://roscoff-culture-collection.org/protocols/media-recipes). Diatom proliferation was prevented in some cultures by the addition of GeO_2 (Sigma-Aldrich, St-Quentin-Fallavier, France) at 9.6 μM.

Isolation from enriched samples was performed by single cell pipetting or by FCM cell sorting (Marie et al., 2017). A FACSAria® cytometer (Becton Dickinson, San José, CA, USA) equipped with a 488-nm laser was used for cell sorting. Acquisition was triggered on red fluorescence and sorting was performed in "single cell" mode using 20 PSI as sheath pressure. Filtered seawater (0.22 μm) was used as sheath fluid. Cells were sorted into 48-well plates containing 1 mL of L1 medium supplemented with 0.01% bovine serum albumin. Three days after sorting, a mixture of penicillin, neomycin, and streptomycin (PNS, Ref P4083; Sigma) was added to each well at a final concentration of 0.1%. Cell growth was monitored by flow cytometry and microscopy after 2 weeks.

For serial dilution either 500 or 50 μL of water sample was added to 15 mL of L1. Then, 24 wells of a Greiner Bio-One™ 96 Deep Well plate (Dominique Dustscher, Brumath, France) were filled with 0.5 mL of each dilution. Wells were later screened by optical microscopy and with a Guava® (Merck, Darmstadt, Germany) flow cytometer. Unialgal wells were transferred to ventilated T-25 CytoOne® flasks (Starlab, Orsay, France) with 15 mL of L1 media.

All cultures were incubated at 4°C with a 12:12 light–dark cycle and transferred to new medium once a month. Light intensity was approximately 100 μmole photons.m^{-2}.s^{-1}. The isolation method, culture medium and environmental conditions for each strain are reported in Supplementary Data S1.

Cultures were screened and de-replicated by optical microscopy and partial 18S rRNA sequences (see below). We aimed to keep, whenever possible, one strain of each taxon per sampling day and per depth. After de-replication, 416 strains were added to the Roscoff Culture Collection (http://www.roscoff-culture-collection.org) of which 276 were chosen to be described in this paper based on 18S rRNA sequence quality and reliability of culture growth.

Molecular analyses

Strains were identified using partial 18S rRNA sequences. DNA was extracted directly from the cultures by a simple heating cycle of 95°C for 5 min, prior to PCR. A DNA

extraction with NucleoSpin Plant II kit (Macherey-Nagel) was performed following the manufacturer's instructions for thick-walled or low concentration strains. For 18S rRNA amplification the primers 63F (5'-ACGC-TTGTCTCAAA-GATTA-3') and 1818R (5'-ACGGAAACCTTGTTACGA-3') (Lepère et al., 2011) were used. PCR amplification was performed in a 10 μL mix containing 5 μL of Phusion High-Fidelity PCR Master Mix® 2×, 0.3 μM final concentration of primer 63F, 0.3 μM final concentration of primer 1818R, 1 μL of DNA and H_2O. Thermal conditions were: 98°C for 5 min, followed by 35 cycles of 98°C for 20 s, 55°C for 30 s, 72°C for 90 s, and a final cycle of 72°C for 5 min. The PCR products were sent for sequencing at Macrogen Europe (https://dna.macrogen-europe.com) using the internal primer 528F (5'-CCGCGGTAATTCCAGCTC-3') (Zhu et al., 2005).

Partial sequences were compared with those available in Genbank using the BLAST plugin in Geneious 10 (Kearse et al., 2012). Sequences were aligned using the ClustalW2 (Larkin et al., 2007) plugin in Geneious 10 and grouped into phylotypes with 100% sequence similarity. Phylotypes represented by more than one strain are listed in Supplementary Data S1. Depending on general sequence quality, partial 18S rRNA sequence alignments were built for each group, including: 49 sequences with 436 nucleotide positions for pennate diatoms, 36 sequences with 612 positions for centric diatoms, 27 sequences with 392 positions for other members of the Heterokontophyta, 52 sequences with 361 positions for Chlorophyta, 10 sequences with 638 positions for Cryptophyta, 11 sequences with 692 positions for Haptophyta, and 6 sequences with 372 positions for Alveolata (Dinophyta). Phylogenetic trees were built using FastTree v2.1.11 (Price et al., 2010) as implemented in Geneious 10. Alignments are available from https://github.com/vaulot/Paper-2019-Ribeiro-GE-cultures.

Microscopy

One strain per phylotype representative of the 18S rRNA genetic diversity was chosen for optical light microscopy (LM). Using a Nikon Eclipse 80i (Nikon) with a 100× objective and differential interference contrast, pictures of live cultures were captured with a SPOT digital camera (Diagnostics Instruments, Sterling Heights, MI, USA).

Results

In the present study, partial 18S rRNA gene sequences and light microscopy were used to characterize 276 Arctic strains obtained during the Green Edge campaign (Supplementary Data S1), 77 and 199 isolated from ice and water samples, respectively (**Figure 2**). By combining different pre-isolation and isolation techniques we were able to retrieve 276 strains assigned to 57 phylotypes characterized by 100% similarity of partial 18S rRNA sequencing. A significant level of novelty exists within these strains, as almost 60% of the representative sequences of phylotypes did not match any sequence from previously cultured strains (**Table 1**) and more than 40% did not match any existing sequence from environmental datasets. The sequence of one strain (**RCC5319**) had only a 95.3% match to any existing sequence. Strains belonged

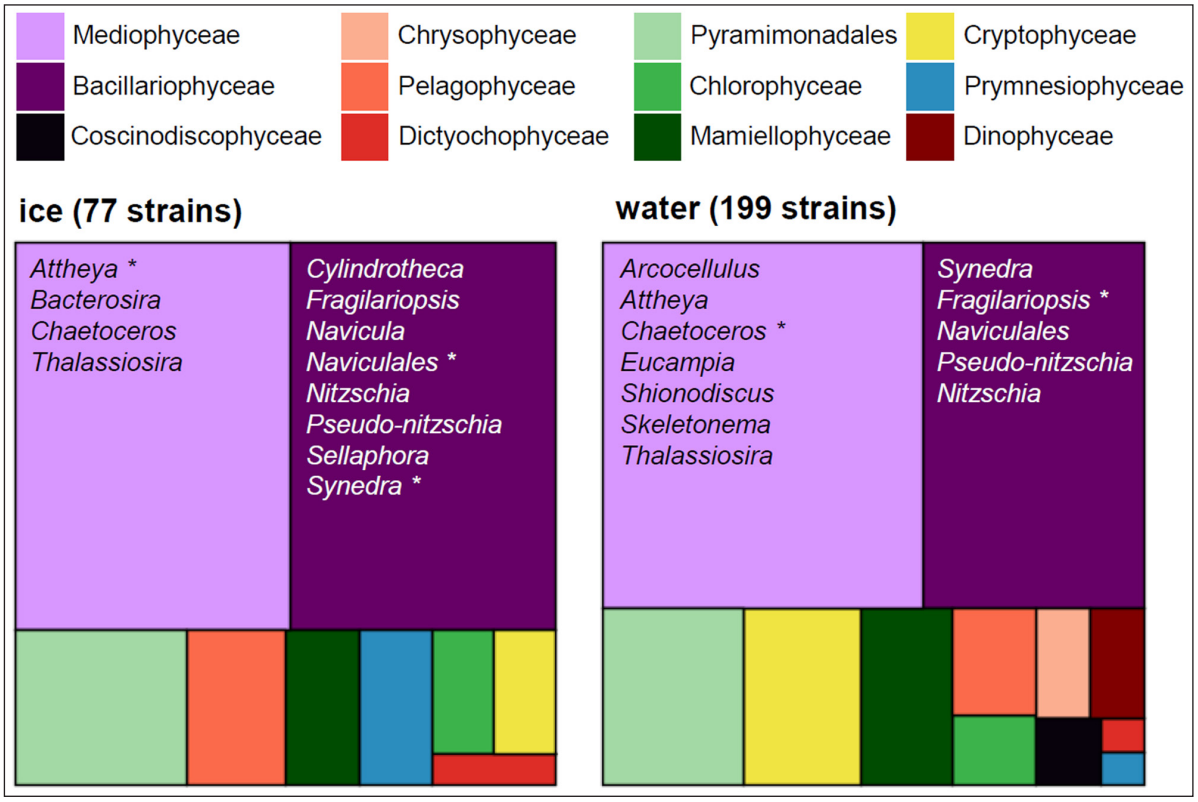

Figure 2: Overall diversity of strains. Overall diversity of the strains retrieved from sea ice and water samples assigned at the class level. Most abundant diatom genera strains are marked with an asterisk. DOI: https://doi.org/10.1525/elementa.401.f2

to 5 divisions (**Table 2**): Heterokontophyta (208), Chlorophyta (44), Cryptophyta (16), Haptophyta (4), and Dinophyta (4). Diatoms were by far the most abundant group (193), with the genera *Chaetoceros* (42) and *Attheya* (40), followed by *Synedra* (23), *Thalassiosira* (18), Naviculales (18) and *Fragilariopsis* (17), being the most represented. The flagellates *Baffinella* (13) and *Pyramimonas* (24) were the most abundant non-diatom genera. With 10 strains, *Micromonas polaris* dominated picoplanktonic isolates, although one strain of *Bathycoccus prasinos* was also isolated. Four strains of dinoflagellates assigned to the genus *Biecheleria* were retrieved from samples from the *Amundsen* cruise. The level of novelty varied between the different taxonomic groups and, for some classes such as Chlorophyceae and Cryptophyceae, we did not recover any strains corresponding to novel 18S rRNA sequences (Figure S1).

Phylogenetic analysis of culture diversity

Diatoms – Bacillariophyceae

The *Cylindrotheca* sp. phylotype represented by **RCC5303** contains two strains from ice core samples from the pre-bloom and bloom-development phases (Supplementary Data S1). Cells are solitary with two chloroplasts, a long apical (>35 μm) and short transapical axis (~3 μm) (**Figure 3R**). *Cylindrotheca* is a genus frequently observed in the Arctic, mainly represented by the cosmopolitan species complex *C. closterium* (Lovejoy et al., 2002; Li et al., 2007; Katsuki et al., 2009; Poulin et al., 2011). However, sequences from the strains obtained in this study branched apart from *C. closterium* (**Figure 4**), but grouped with 100% identity with an uncultured *Cylindrotheca* sequence from the Arctic (GenBank JF698839). The sequence of *Cylindrotheca* sp. **RCC5216**, also isolated from an IC ice core sample (Supplementary Data S1), differed from that of *Cylindrotheca* sp. **RCC5303** by two base pairs. Cells of **RCC5216** are curved to sigmoid, forming coarse aggregates, with 17–20 μm apical and ~4 μm transpical axes (**Figure 3B**).

Table 1: Level of novelty of the different phylotypes based on BLAST analysis of 18S rRNA against Genbank nr database (Supplementary Data S2). DOI: https://doi.org/10.1525/elementa.401.t1

Phylotype novelty[1]	Number of phylotypes
previously cultured	24
previously observed but not cultured	9
not previously observed	24

[1] "previously cultured" indicates phylotypes with 18S rRNA sequences that are 100% similar to that of a previously isolated culture, "previously observed but not cultured" indicates phylotypes with 18S rRNA sequences that are 100% similar to that of a sequence detected in the environment but for which no culture existed prior to this work, and "not previously observed" indicates phylotypes for which no 100% similar 18S rRNA sequence had been detected previously in the environment.

Table 2: Number of strains obtained from water and sea ice samples for each genus. DOI: https://doi.org/10.1525/elementa.401.t2

Strain assignation	Water	Ice
Chlorophyta		
Bathycoccus	0	1
Chlamydomonas	4	2
Mantoniella	2	1
Micromonas	9	1
Pyramimonas	17	7
Cryptophyta		
Rhodomonas	3	0
Baffinella	11	2
Dinophyta		
Biecheleria	4	0
Haptophyta		
Isochrysis	0	3
Pseudohaptolina	1	0
Heterokontophyta		
Actinocyclus	2	0
Arcocellulus	3	0
Attheya	27	13
Bacterosira	0	1
Chaetoceros	36	6
Coscinodiscus	1	0
Cylindrotheca	0	3
Dinobryon	1	0
Eucampia	1	0
Fragilariopsis	14	3
Navicula	0	2
Naviculales	10	8
Nitzschia	4	3
Pedinellales	0	1
Pelagophyceae	6	4
Pseudo-nitzschia	8	1
Sellaphora	0	1
Shionodiscus	2	0
Skeletonema	1	0
Spumella	3	0
Synedra	18	5
Synedropsis	1	1
Thalassiosira	10	8

Figure 3: Light microscopy images of diatom strains. Light microscopy images from diatoms strains retrieved during Green Edge 2016 campaign. Size bars correspond to 10 μm. **A)** *Chaetoceros neogracilis* strain RCC5210; **B)** *Cylindrotheca* sp. strain RCC5216; **C)** *Chaetoceros gelidus* strain RCC5266 forming a small chain; **D)** *Synedropsis hyperborea* strain RCC5291; **E)** *Thalassiosira* sp. strain RCC5327; **F)** *Bacterosira bathyomphala* strain RCC5328 in both girdle and valve view; **G)** *Thalassiosira* cf *antarctica* strain RCC5348 valve with fine radiating areolae; **H)** *Thalassiosira* sp. strain RCC5350 in girdle view; **I)** *Navicula* sp. strain RCC5373; **J)** *Navicula ramosissima* strain RCC5374; **K)** Naviculales sp. RCC5387 cell in valve view; **L)** *Nitzschia* sp. strain RCC5389; **M)** *Nitzschia* sp. RCC5390 cells in ribbon-like colonies; **N)** *Nitzschia* sp. strain RCC5391; **O)** Naviculales strain RCC5402; **P)** *Nitzschia* sp. strain RCC5458; **Q)** *Sellaphora* sp. strain RCC5460; **R)** *Cylindrotheca* sp. strain RCC5463; **S)** *Pseudo-nitzschia arctica* strain RCC5469; **T)** *Nitzschia* sp. strain RCC5489; **U)** *Fragilariopsis cylindrus* strain RCC5501; **V)** *Skeletonema* sp. strain RCC5502; **W)** *Nitzschia* sp. strain RCC5510; **X)** *Arcocellulus* sp. strain RCC5530; **Y)** *Eucampia groenlandica* strain RCC5531; **Z)** *Shionodiscus bioculatus* strain RCC5532; **AA)** *Synedra* sp. strain RCC5535; **AB)** *Attheya longicornis* strain RCC5555 solitary cell in girdle view; **AC)** Naviculales sp. RCC5564 forming a small chain; **AD)** *Attheya septentrionalis* strain RCC5567; **AE)** *Thalassiosira rotula* RCC5605; **AF)** *Chaetoceros decipiens* strain RCC5606 forming a small, curved chain; **AG)** *Actinocyclus* sp. RCC5608; **AH)** *Shionodiscus bioculatus* strain RCC5609. DOI: https://doi.org/10.1525/elementa.401.f3

The *Fragilariopsis cylindrus* phylotype represented by **RCC5501** groups 17 strains originating from all main sampling sites, substrates and phases of the bloom (Supplementary Data S1). The 18S rRNA sequence matched with 100% similarity the Arctic *F. cylindrus* strain RCC4291 (**Figure 4**), a known cold-adapted diatom (Mock et al., 2017), used as an indicator of polar water and ice (Quillfeldt, 2004). Cells have a short apical axis (~4 μm), rounded ends, and a transapical axis of approximately 3 μm length (**Figure 3U**).

Navicula ramosissima strain **RCC5373** was retrieved from an ice core sample from the pre-bloom period and shared 100% similarity with *Navicula ramosissima* strain TA439 from the Yellow Sea and *Navicula* sp. strain ECT3499 obtained from the skin of Florida manatees (**Figure 4**). Cells are solitary, lanceolate, with apical and transpical axes of ~25 μm and 7 μm, respectively, two elongated chloroplasts on each side of the girdle, and large lipid bodies (**Figure 3I**). Interestingly, none of the *Navicula* spp. strains recovered in this study were related to previous polar strains or environmental sequences, despite this genus being diverse (Katsuki et al., 2009) and abundant in the Arctic (Poulin et al., 2011; Kauko et al., 2018).

Navicula sp. strain **RCC5374** was recovered from an ice core sample from the bloom-development phase. The sequence of this strain is not very closely related to those of previously reported polar *Navicula*, but is 99.2% similar to strain **RCC5373** and 99.7% similar to strain KSA2015-19 from the Red Sea (**Figure 4**). Cells have a ~25 μm apical axis, slightly radiating valvar striae and rostrate ends (**Figure 3J**).

The Naviculales phylotype represented by **RCC5564** contains 12 strains from all phases and sampling sites (Supplementary Data S1). Its sequence is 99.7% similar to Naviculales strain CCMP2297 from northern Baffin Bay and to uncultured sequences from the Arctic (**Figure 4**). Cells have ~3 μm apical and 5 μm pervalvar axes. They are solitary or form short chains (**Figure 3AC**).

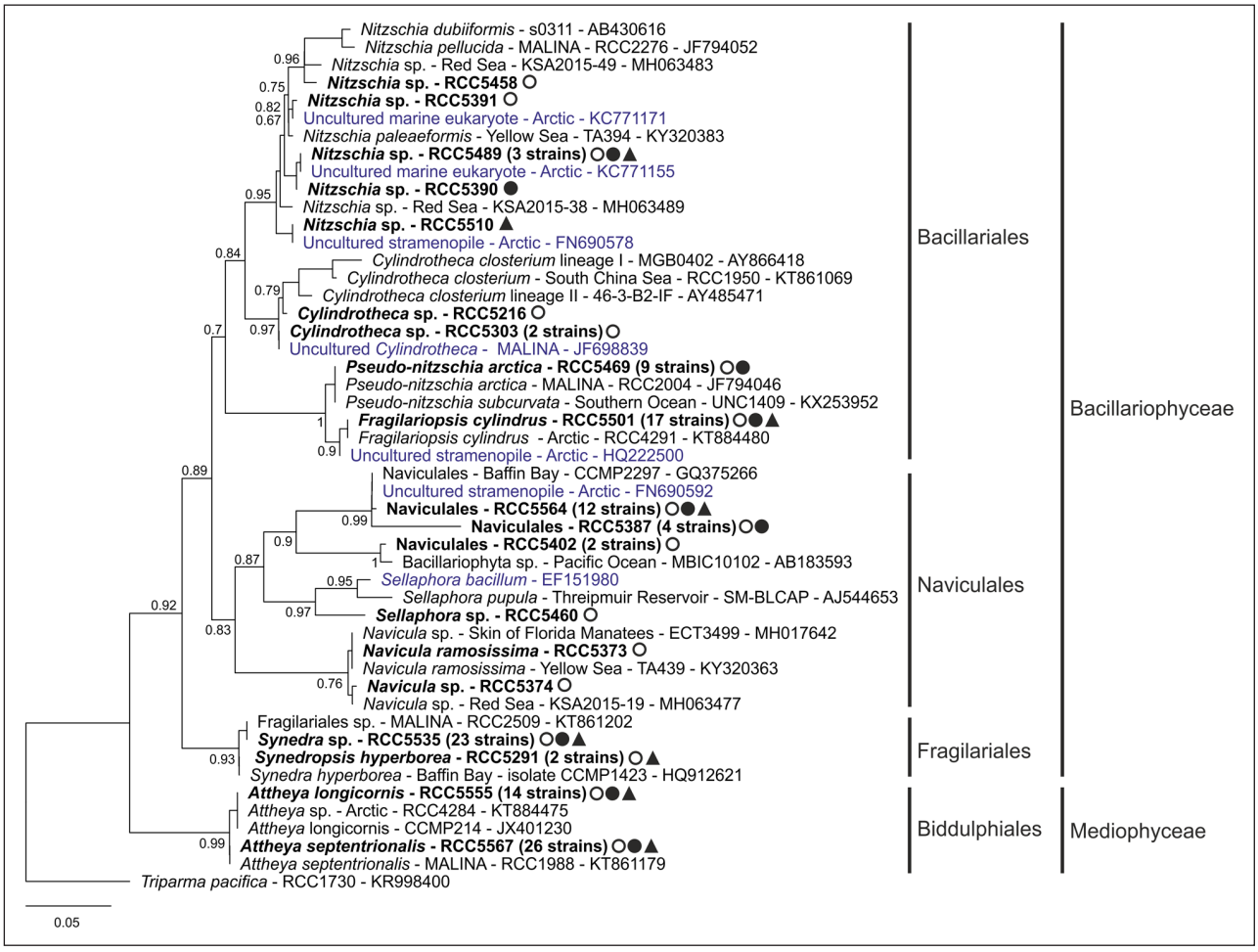

Figure 4: The 18S rRNA phylogenetic tree of pennate diatoms. The 18S rRNA phylogenetic tree inferred by FastTree approximate-maximum-likelihood for pennate diatom strains obtained during the Green Edge campaign (in bold), using an alignment of 49 sequences with 436 nucleotide positions. Circles mark strains retrieved from the Ice Camp sea ice (open) and water samples (solid); triangles (solid) mark *Amundsen* cruise water samples. The origin, sampling substrate, and phase of the bloom from which they were recovered are provided along with their names and RCC code in Supplementary Data S1. When one phylotype is represented by more than one strain, the number of strains is indicated between parenthesis. For the reference sequences, the strain (whenever available) and the Genbank ID number are displayed. Environmental sequences are marked in blue. DOI: https://doi.org/10.1525/elementa.401.f4

The Naviculales phylotype represented by **RCC5387** contains four strains from IC water and ice samples (Supplementary Data S1). Its sequence has low similarity to sequences from GenBank or to the phylotype represented by **RCC5564**, sharing only 96.9% similarity with strain CCMP2297 (Naviculales) (**Figure 4**). Cells are elongated, mainly solitary, with up to 6 μm apical and 3 μm pervalvar axes (**Figure 3K**).

The Naviculales phylotype represented by **RCC5402** has two strains, both retrieved from IC ice cores during the pre-bloom period (Supplementary Data S1). Their sequence shares 99.2% identity with the Bacillariophyta MBIC10102 strain from the Pacific Ocean and groups with Naviculales sequences with strong bootstrap support (91%, **Figure 4**). Cells are small ~4 μm long and 2 μm wide, sometimes solitary, but mainly forming large aggregates (**Figure 3O**).

The *Nitzschia* sp. phylotype represented by **RCC5489** contains three strains from both sampling sites and substrates (Supplementary Data S1). Its sequence has no close similarity to any GenBank sequence from strains besides **RCC5390** (**Figure 4**). Cells are ~11 μm wide, mainly solitary or forming small aggregates (**Figure 3L**). Members of the genus *Nitzschia* are often reported to thrive in the Arctic (Johnsen et al., 2018; Kauko et al., 2018), with *Nitzschia frigida*, for example, being considered as the single most important diatom associated with sea ice (Rózanska et al., 2009; Leu et al., 2015). Surprisingly, none of the *Nitzschia* spp. strains isolated in this study had high 18S rRNA similarity to other known polar strains. They did, however, have high similarity with Arctic environmental sequences (**Figure 4**).

Nitzschia sp. **RCC5390** was retrieved from an IC pre-bloom sample (Supplementary Data S1) and its sequence is the closest to **RCC5489** (99.8% similarity, **Figure 4**). Cells have 7 μm apical axis and 5 μm pervalvar distance, forming ribbon-like colonies (**Figure 3M**).

Nitzschia sp. **RCC5391** was isolated from an ice core sample during the pre-bloom period. Its sequence matches with only 97.8% similarity that of a strain TA394 (*Nitzschia paleaeformis*) from the Yellow Sea (**Figure 4**). Cells are solitary lanceolate with bluntly rounded apices, measuring ~10 μm and 2 μm for the apical and transapical axes, respectively (**Figure 3N**).

Nitzschia sp. **RCC5458** was also retrieved from an ice sample from the pre-bloom period and its sequence is 98.1% similar to *Nitzschia* sp. strain KSA2015-49 from the Red Sea (**Figure 4**). Cells are linear to lanceolate and larger than other *Nitzschia* strains retrieved in this study, with an apical axis up to 15 μm (**Figure 3P**).

Nitzschia sp. **RCC5510** was isolated from AM waters (Supplementary Data S1). Its sequence is 98.6% similar to *Nitzschia* sp. strain KSA2015-38 from the Red Sea (**Figure 4**). It is the only strain from this genus recovered only from AM. Its sequence branches apart from all other *Nitzschia* sp. (**Figure 4**). Cells are almost round in the valvar view and rather small (apical axis ~4 μm) compared to the other *Nitzschia* strains isolated here (**Figure 3W**).

The *Pseudo-nitzschia arctica* phylotype represented by **RCC5469** contains nine strains of the recently described *P. arctica* (Percopo et al., 2016), all originating from IC (Supplementary Data S1). Their sequence is 100% similar to *P. arctica* RCC2004 (**Figure 4**), a potentially endemic species with a wide distribution in the Arctic (Percopo et al., 2016; Balzano et al., 2017). Only solitary cells were observed, with lanceolate shape in valvar view, measuring ~50 μm and 3 μm for the apical and transapical axes, respectively (**Figure 3S**).

Sellaphora sp. strain **RCC5460** was retrieved during pre-bloom from an IC ice core sample. Its sequence matches with 99% similarity that of the freshwater *Sellaphora pupula* strain SM-BLCAP (**Figure 4**). Cells are small, with 5 μm apical and 4 μm pervalvar axes, solitary or forming aggregates (**Figure 3Q**). *S. pupula* is a species complex containing many pseudo- and semi-cryptic representatives capable of thriving in a wide range of environmental conditions (Poulíčková et al., 2008). Further molecular/morphological analyses are needed to properly assign this phylotype.

The *Synedropsis hyperborea* phylotype represented by **RCC5291** contains only two strains, from both IC and AM (Supplementary Data S1). Its sequence shares 100% similarity with *S. hyperborea* strain CCMP1423 (**Figure 4**), although members of the Fragilariaceae are not well resolved by 18S rRNA (Balzano et al., 2017). Cells are solitary or in pairs, exhibiting great variability in shape, which is attributed to vegetative cell division (Hasle et al., 1994). The apical axis is ~14 μm (**Figure 3D**). *S. hyperborea* is an Arctic species with circumpolar distribution, often found in association with sea ice and as an epiphyte of *Melosira arctica* (Hasle et al., 1994; Assmy et al., 2013).

The *Synedra* sp. phylotype represented by **RCC5535** comprises twenty-three strains of which fifteen were isolated from the AM and the other eight from within or under the IC ice (**Figure 4**). Its sequence shares 100% identity with other Arctic strains such as Fragilariales RCC2509. Cells vary considerably in shape, from almost linear to lanceolate and sometimes asymmetrical in the valvar central area. Apical and transapical axes are ~13 μm and 3 μm, respectively (**Figure 3AA**).

Diatoms – Coscinodiscophyceae

The *Actinocyclus* sp. phylotype represented by **RCC5608** comprises two strains isolated from AM waters (Supplementary Data S1). Its sequence shares 100% similarity with a clone from the Arctic (EU371328), and 99.8% with the *Actinocyclus* sp. MPA-2013 isolate from the Pacific Ocean (**Figure 5**). Cells have a pervalvar axis (13–17 μm) longer than the valvar diameter (~5 μm) and discoid chloroplasts (**Figure 3AG**). Although sometimes spotted in low abundance (Katsuki et al., 2009; Crawford et al., 2018), this genus may dominate phytoplankton biomass in Arctic spring blooms (Lovejoy et al., 2002).

Coscinodiscus sp. strain **RCC5319** was isolated from an IC under-ice sample at the peak of the bloom (Supplementary Data S1). The sequence is only 95% similar to that of *C. jonesianus* isolate 24VI12 (KJ577852) (**Figure 5**). Unfortunately, this strain was lost and no images are available. *Coscinodiscus* may be abundant

under the ice pack (Duerksen et al., 2014) and is often reported in Arctic diversity studies (Booth et al., 2002; Lovejoy et al., 2002).

Diatoms – Mediophyceae

The *Arcocellulus* sp. phylotype represented by **RCC5530** contains three strains isolated from 17-m depth from the AM (Supplementary Data S1). Their sequence is 100% similar to RCC2270 *Arcocellulus cornucervis* (**Figure 5**). However, 18S rRNA sequences do not have enough resolution to separate *Arcocellulus* sp. from closer groups such as *Minutocellulus* sp. (Balzano et al., 2017), requiring further analyses for proper assignation. Cells are small (~5 μm) and solitary (**Figure 3X**). The cold-adapted *A. cornucervis* has been reported to be part of the protist community in the Arctic (Blais et al., 2017), including in Baffin Bay in early summer (Lovejoy et al., 2002).

The *Attheya septentrionalis* phylotype represented by **RCC5567** comprises 26 strains from all substrates and sampling sites, from bloom-development and bloom-peak phases (Supplementary Data S1). Their sequence shares 100% similarity with the Arctic strain RCC1988 (**Figure 5**). Cells are lightly silicified with ~6 μm pervalvar axis and horns up to two times the cell length. They are either solitary or form big aggregates (**Figure 3AD**). *A. septentrionalis* is often reported in abundance in Arctic waters and ice (Assmy et al., 2013; Balzano et al., 2017), outcompeting pennate diatoms in high-luminosity/low nutrient conditions (Campbell et al., 2017).

The *Attheya longicornis* phylotype represented by **RCC5555** contains 14 strains, 11 of which were retrieved from AM water samples (Supplementary Data S1). Sequences are 100% identical to the Arctic *A. longicornis* strains RCC4284 and CCMP214 (**Figure 5**). Cells are often solitary or in short chains, with horns up to three times the length of the pervalvar axis (**Figure 3AB**). Together with *A. septentrionalis*, *A. longicornis* can comprise a significant portion of the diatom community in Arctic sea ice (Campbell et al., 2017).

Bacterosira bathyomphala strain **RCC5328** was retrieved from an ice core sample and its sequence shares 99.8% identity with the Arctic *Bacterosira* sp. RCC4297 and with *B. bathyomphala* strain NB04-B6 from an estuary (**Figure 5**). Cells (~9 μm pervalvar axis) form short and tight chains with contiguous valves (**Figure 3F**). *B. bathyomphala* is often reported in northern and polar waters (Crawford et al., 2018; Johnsen et al., 2018), especially where silicate concentration is high (Luddington et al., 2016).

The *Chaetoceros neogracilis* phylotype represented by **RCC5210** contains 33 strains retrieved from all sites, substrates and phases of the bloom (Supplementary Data S1). Its sequences share 100% similarity with polar *C. neogracilis* strains (e.g. RCC2506). The 18S rRNA gene does not, however, have enough resolution to differentiate within *C. neogracilis* clades (Balzano et al., 2017). Cells are small, solitary or forming aggregates, with the pervalvar axis slightly longer than the valvar diameter (4 μm) (**Figure 3A**). The genus *Chaetoceros* is abundant in temperate and polar waters (Lovejoy et al., 2002; Malviya et al., 2016) and *C. neogracilis* dominates the nanophytoplankton community in surface waters in the Beaufort Sea in the summer (Balzano et al., 2012a).

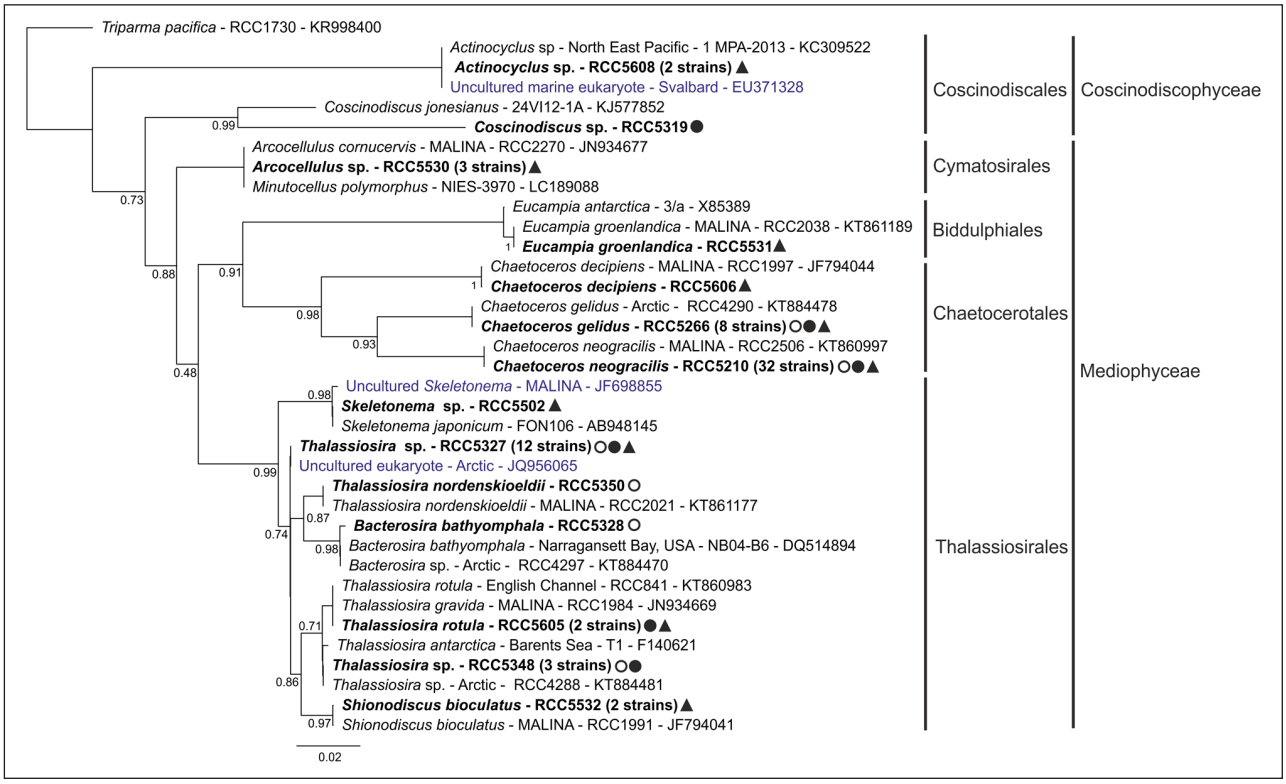

Figure 5: The 18S rRNA phylogenetic tree of centric diatoms. The 18S rRNA phylogenetic tree inferred by FastTree approximate-maximum-likelihood analysis for centric diatom strains. Legend as in Figure 4, using an alignment of 36 sequences with 612 nucleotide positions. DOI: https://doi.org/10.1525/elementa.401.f5

The *Chaetoceros gelidus* phylotype represented by **RCC5266** contains eight strains from all substrates and sampling sites, but only from the bloom-development and bloom-peak periods (Supplementary Data S1). Their sequences were 100% similar to those of the Arctic strains RCC4290 and RCC1992 (**Figure 5**). Cells are rectangular (~6 μm), forming small, tight chains with narrow apertures and long inner setae, up to 25 μm (**Figure 3C**). *C. gelidus* is a recently described species, previously considered as a *Chaetoceros socialis* ecotype, and is characteristic of northern temperate and polar waters (Chamnansinp et al., 2013). It is reported to form blooms (Booth et al., 2002) and can represent an important fraction of diatom abundance and biomass in Baffin Bay (Crawford et al., 2018).

Chaetoceros decipiens strain **RCC5606** was isolated from 30-m depth in AM water (Supplementary Data S1). Its sequence is 99.8% similar to Arctic strain *C. decipiens* RCC1997 (**Figure 5**). Cells (~10–30 μm apical axis) have very long inner setae (>100 μm) and form short, semicircular colonies (**Figure 3AF**), which contrasts with previous morphological descriptions of *C. decipiens* (Hasle and Syvertsen, 1997; Balzano et al., 2017), indicating that it might correspond to a new phylotype. This cosmopolitan species has frequently been reported in the Arctic, both in ice and open waters (Lovejoy et al., 2002; Joo et al., 2012; Johnsen et al., 2018).

Eucampia groenlandica **RCC5531** strain was retrieved from 30 m depth during the *Amundsen* cruise. Its sequence shares 100% similarity with *E. groenlandica* Arctic strain RCC2038 (**Figure 5**). Cells are lightly silicified with varying sizes, forming straight or moderately curved colonies (**Figure 3Y**). *E. groenlandica* was first reported in Baffin Bay (Cleve, 1896) although its distribution is not constrained to the Arctic (Lee and Lee, 2012).

The *Shionodiscus bioculatus* phylotype represented by **RCC5532** contains two strains isolated from the AM (Supplementary Data S1). Its sequence shares 99.8% similarity with *S. bioculatus* strain RCC1991 from the Beaufort Sea (**Figure 5**). The morphology of the two strains differs (**Figure 3Z** and **AH**): **RCC5532** cells have a longer pervalvar axis (~32 μm), shorter valve diameter and fewer discoid chloroplasts in comparison to **RCC5609**. Isolates with identical 18S rRNA may present cryptic diversity based on ITS divergence (Luddington et al., 2016). *S. bioculatus* is reported as dominating the top portion of submerged sea-ice ridges (Fernández-méndez et al., 2018).

Skeletonema sp. **RCC5502** strain was retrieved during the AM and its sequence shared 100% similarity with *Skeletonema japonicum* from Onagawa Bay and 99.7% with an Arctic environmental sequence (JF698855, **Figure 5**). Cells are small (5 μm diameter) with a very short pervalvar axis ~3 μm, being either solitary or in pairs (**Figure 3V**). The genus *Skeletonema* has been reported from high latitude, winter samples (Eilertsen and Degerlund, 2010) and *S.* aff. *japonicum* seems to thrive in polar environments with low silicate concentration (Luddington et al., 2016).

The *Thalassiosira* sp. phylotype represented by **RCC5327** contains 12 strains from all sampling sites, substrates and phases of the bloom (Supplementary Data S1). The best match to its sequence is from an Arctic environmental sequence (99.5% similarity), branching apart from other *Thalassiosira* clades (**Figure 5**). It shares 99.2% identity with *T. nordenskioeldii* strain RCC2021. Cells are small (<8 μm diameter) with a long pervalvar dimension relative to valve size and long (>20 μm) marginal threads (**Figure 3E**).

The *Thalassiosira* sp. phylotype represented by **RCC5348** contains three strains from IC water and ice. Its sequence is 99.8% similar with a *T. antarctica var. borealis* isolate from the Barents Sea (**Figure 5**). Cells are cylindrical with a short pervalvar axis, a 17–22 μm valvar diameter, and contain fine areolae radiating from the valve center (**Figure 3G**). *T. antarctica* is reported in coastal and ice-edge cold waters (Hasle and Heimdal, 1968) and associated with high-nutrient concentrations (Luddington et al., 2016).

The sequence of *Thalassiosira nordenskioeldii* strain **RCC5350** isolated from an ice core sample is (100%) identical to that of *T. nordenskioeldii* Arctic strain RCC2021 (**Figure 5**). Cells are cylindrical, either solitary or forming colonies, with a ~6 μm valvar diameter and a 10 μm pervalvar axis, with long processes (**Figure 3H**). *T. nordenskioeldii* is widely distributed in North Atlantic cold, temperate and polar waters (Crawford et al., 2018; Johnsen et al., 2018), often associated with ice (Luddington et al., 2016).

The *Thalassiosira rotula* phylotype represented by **RCC5605** contains two strains, one isolated during the *Amundsen* cruise and one from under-ice at the ice camp during the bloom peak (Supplementary Data S1). The sequence from this phylotype had 100% similarity with those of *T. rotula* strains from the Arctic and the English Channel, but also with that of *Thalassiosira gravida* (RCC1984) (**Figure 5**). 18S rRNA is not a good marker to discriminate between *T. rotula*, a known cosmopolitan species (Hasle and Syvertsen, 1997; Whittaker et al., 2012), and the bipolar *T. gravida* (Balzano et al., 2017). Cells are mainly solitary, with a ~6 μm valvar diameter and a 10–13 μm pervalvar axis with several long marginal threads (**Figure 3AE**).

Other Heterokontophyta

Dinobryon faculiferum strain **RCC5261** was isolated from 1.5 m depth in IC waters from the peak of the bloom (Supplementary Data S1). Its sequence shares 100% similarity to those of other Arctic strains, such as RCC2294 (**Figure 6A**). Cells are solitary with a ~4 μm diameter lorica and long spines (>25 μm) (**Figure 7C**). *D. faculiferum* is a frequently observed mixotroph in Arctic surface waters (Lovejoy et al., 2002; Balzano et al., 2012) that can be found encysted in the top section of ice cores (Kauko et al., 2018), although it is not restricted to polar environments (Unrein et al., 2010).

Spumella sp. **RCC5513** strain isolated from an AM sample branches with *D. faculiferum* and its sequence is 99.8% similar to those of *Spumella* sp. strains from the Baltic Sea (isolate IOW91) and the Atlantic Ocean (RCC4558) (**Figure 6A**). Cells are colorless and solitary, round or slightly elongated with 4 μm diameter and 5 μm flagella (**Figure 7N**). Heterotrophic flagellates from the genus *Spumella* have been previously reported in the Arctic (Lovejoy et al., 2006) and are mostly cold-adapted and associated with lower salinities (Grossmann et al., 2015).

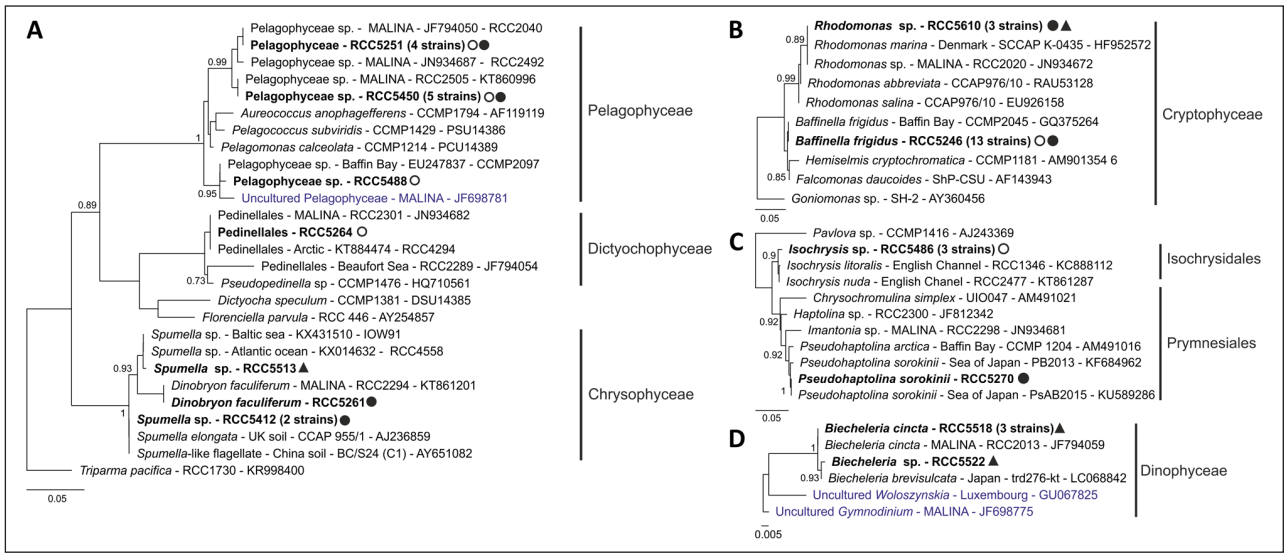

Figure 6: The 18S rRNA phylogenetic tree of other taxonomic groups. The 18S rRNA phylogenetic tree inferred by FastTree approximate-maximum-likelihood analysis for the strains obtained during the Green Edge campaign (in bold) for: **A)** Cryptophyta, using an alignment of 10 sequences with 638 positions; **B)** Heterokontophyta, alignment of 27 sequences with 392 positions; **C)** Haptophyta, using an alignment of 11 sequences with 692 positions and **D)** Dinophyta, alignment of 6 sequences with 372 positions. Legend as in Figure 4. DOI: https://doi.org/10.1525/elementa.401.f6

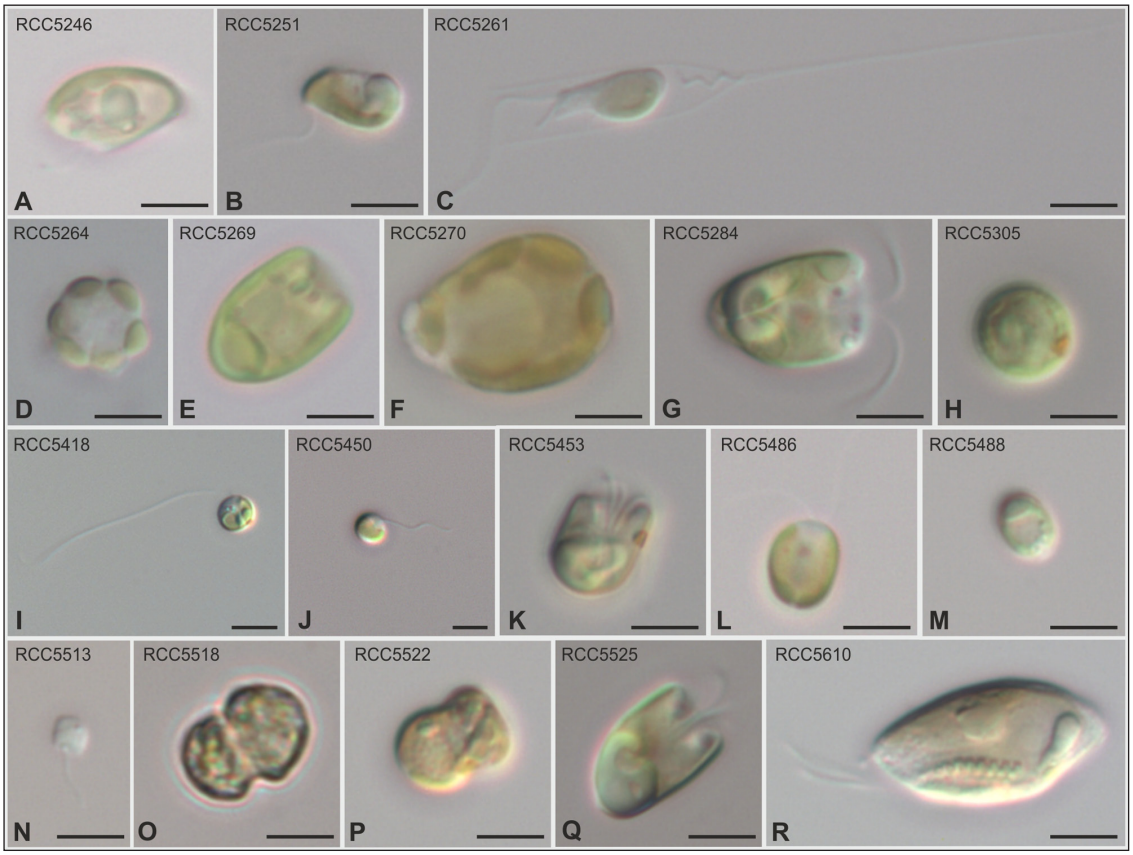

Figure 7: Light microscopy images of flagellate strains. Light microscopy of selected strains of flagellates obtained during Green Edge 2016 campaign. Size bars correspond to 5 μm. **A)** *Baffinella frigidus* sp. strain RCC5246; **B)** Pelagophyceae strain RCC5251; **C)** *Dinobryon faculiferum* strain RCC5261; **D)** Pedinellales RCC5264 cell showing a ring of six peripheral chloroplasts; **E)** *Pyramimonas australis* strain RCC5269; **F)** *Pseudohaptolina sorokinii* RCC5270; **G)** *Pyramimonas* sp. strain RCC5284; **H)** *Chlamydomonas* sp. strain RCC5305; **I)** *Mantoniella baffinensis* strain RCC5418 with a long flagellum and visible eyespot; **J)** Pelagophyceae strain RCC5450; **K)** *Pyramimonas* sp. strain RCC5453; **L)** *Isochrysis* sp. strain RCC5486; **M)** Pelagophyceae strain RCC5488; **N)** *Spumella* sp. strain RCC5513; **O)** *Biecheleria cincta* strain RCC5518; **P)** *Biecheleria* sp. strain RCC5522; **Q)** *Pyramimonas* sp. strain RCC5525; **R)** *Rhodomonas* sp. RCC5610. DOI: https://doi.org/10.1525/elementa.401.f7

The *Spumella* sp. phylotype represented by **RCC5412** contains two isolates from IC waters. Their sequence is 100% similar to those of *Spumella* sp. isolate CCAP 955/1 from a soil sample collected in China and *Spumella elongata* isolate JBC/S24 from the UK (**Figure 6A**). Interestingly, these sequences are part of a soil sub-cluster within Chrysophyceae clade C with few aquatic representatives (Boenigk et al., 2005). These strains were lost and no images are available.

Pedinellales strain **RCC5264** was retrieved from an IC ice sample at the peak of the bloom (Supplementary Data S1), and its sequence matched with 100% similarity that of the undescribed Pedinellales Arctic strain RCC2301 and also with CCMP2098 isolated from Baffin Bay (GenBank EU247836). Cells are solitary, round in anterior view (6 μm diameter), apple-shaped to slightly elongated in side view, with six peripheral chloroplasts (**Figure 7D**). Further taxonomic analyses are needed to properly assign this strain at the genus level, although its sequence matches with with 98.6% similarity that of a *Pseudopedinella* sp. strain (CCMP1476) from the Sargasso Sea (**Figure 6A**).

The Pelagophyceae phylotype represented by **RCC5450** groups five strains from IC, four from water samples and one from ice (Supplementary Data S1). Its sequence shares 100% similarity with other Arctic strains such as RCC2505 and RCC2515. Cells are round, ~4 μm in diameter, with two flagella of different sizes, ~2 μm and 7 μm, respectively (**Figure 7J**). Pelagophyceae may dominate surface waters during the Arctic summer (Balzano et al., 2012a) and yet undescribed strains have been recovered previously from northern waters (Balzano et al., 2012).

The Pelagophyceae phylotype represented by **RCC5251** contains four strains from the peak of the bloom (Supplementary Data S1) and its representative sequence shares 100% similarity with that of the undescribed Arctic Pelagophyceae RCC2040 (**Figure 6A**). Cells are elongated with ~7 μm in side view (**Figure 7B**).

Pelagophyceae strain **RCC5488**, isolated from an ice sample during bloom-development phase (Supplementary Data S1), has a sequence that branches apart from the other Pelagophyceae phylotypes (**Figure 6A**), matching with 100% similarity another strain isolated from Baffin Bay, CCMP2097. Cells are solitary, ~4 μm in size (**Figure 7M**).

Chlorophyta

The *Chlamydomonas* sp. phylotype represented by **RCC5305** contains 6 strains isolated from IC water and ice samples from the peak of the bloom and is the only representative of the Chlorophyceae in our set of culture isolates (Supplementary Data S1). Its sequence is 100% identical to sequences from the *Chlamydomonas pulsatilla* polar strain CCCryo 038–99, but also strains from Antarctic ice and Arctic fresh water (**Figure 8**), all belonging to the *Polytoma* clade (Pocock et al., 2004). Cells are round or elongated, ~7 μm in diameter or 10 μm long, respectively (**Figure 7H**). *Chlamydomonas* is a common genus found in the Arctic during the spring and summer months (Lovejoy et al., 2002; Balzano et al., 2012a), that can occur in association with sea-ice (Majaneva et al., 2017).

Bathycoccus prasinos **RCC5417** strain was recovered from an IC ice core sample during bloom development (Supplementary Data S1). This genus has recently been observed in Arctic waters (Terrado et al., 2013; Kilias et al., 2014), including during winter (Joli et al., 2017) and has a highly conserved 18S rRNA. Its sequence shares 100% similarity with *B. prasinos* strain CCMP1898 from the Mediterranean Sea (**Figure 8**).

The *Micromonas polaris* phylotype represented by **RCC5239** regroups 10 strains recovered from IC ice and water samples. Its sequence shares 100% similarity with those of the Arctic strains *M. polaris* CCMP2099 and RCC2308 (**Figure 8**). *M. polaris* often dominates the picoplanktonic community in the Arctic (Sherr et al., 2003; Not et al., 2005; Balzano et al., 2012a), and metagenomic data suggest its presence in Antarctic waters (Delmont et al., 2015; Simmons et al., 2015).

Mantoniella baffinensis **RCC5418**, recently described (Yau et al., 2019), was recovered from pre-bloom IC ice core samples. Its sequence branched apart from other known strains (**Figure 8**), matching with 98% similarity the Arctic strains RCC2497 and RCC2288, which were also recently described as *Mantoniella beaufortii* (Yau et al., 2019). Cells are round, ~4 μm in diameter bearing two unequal flagella with a visible red eyespot opposite to the flagella (**Figure 7I**).

Mantoniella sp. strain **RCC5273** was isolated from a sample taken at 20-m depth during the peak of the bloom. Its sequence shared 99.8% similarity with that of *Mantoniella squamata* strain CCAP 1965/1, a cosmopolitan species (Hasle and Syvertsen, 1997) frequently observed in the Arctic (Lovejoy et al., 2007; Majaneva et al., 2017). This strain was lost and no images are available.

Mantoniella sp. strain **RCC5301** was also isolated from 20-m depth during the peak of the bloom and its sequence is not closely related to any strain or environmental sequence. However, it clustered together with other *Mantoniella* sequences, sharing 98.3% identity with *M. squamata* CCAP 1965/1 (**Figure 8**). This strain was also lost and no images are available.

The *Pyramimonas diskoicola*/*Pyramimonas gelidicola* phylotype represented by **RCC5525** contains 11 strains from all main sampling sites, substrates, and phases of the bloom (Supplementary Data S1). The sequence from **RCC5525** is 100% similar to that of the Arctic *P. diskoicola* and the Antarctic *P. gelidicola* within the subgenus *Vestigifera* (**Figure 8**). Three types of cell morphology have been observed: pyramidal, elongated, and nearly round. A big starch grain with two lobes surrounds a pyrenoid located at the basal end; large lipid bodies are present near the apical end. Cells are ~7 μm in length and have four flagella with similar size (**Figure 7Q**).

The *Pyramimonas sp.* phylotype represented by **RCC5284** contains 8 strains from the IC during the later phases of the bloom, 7 of which were isolated from water samples (Supplementary Data S1). The representative sequence shares 99.7% similarity with that of *P. diskoicola*

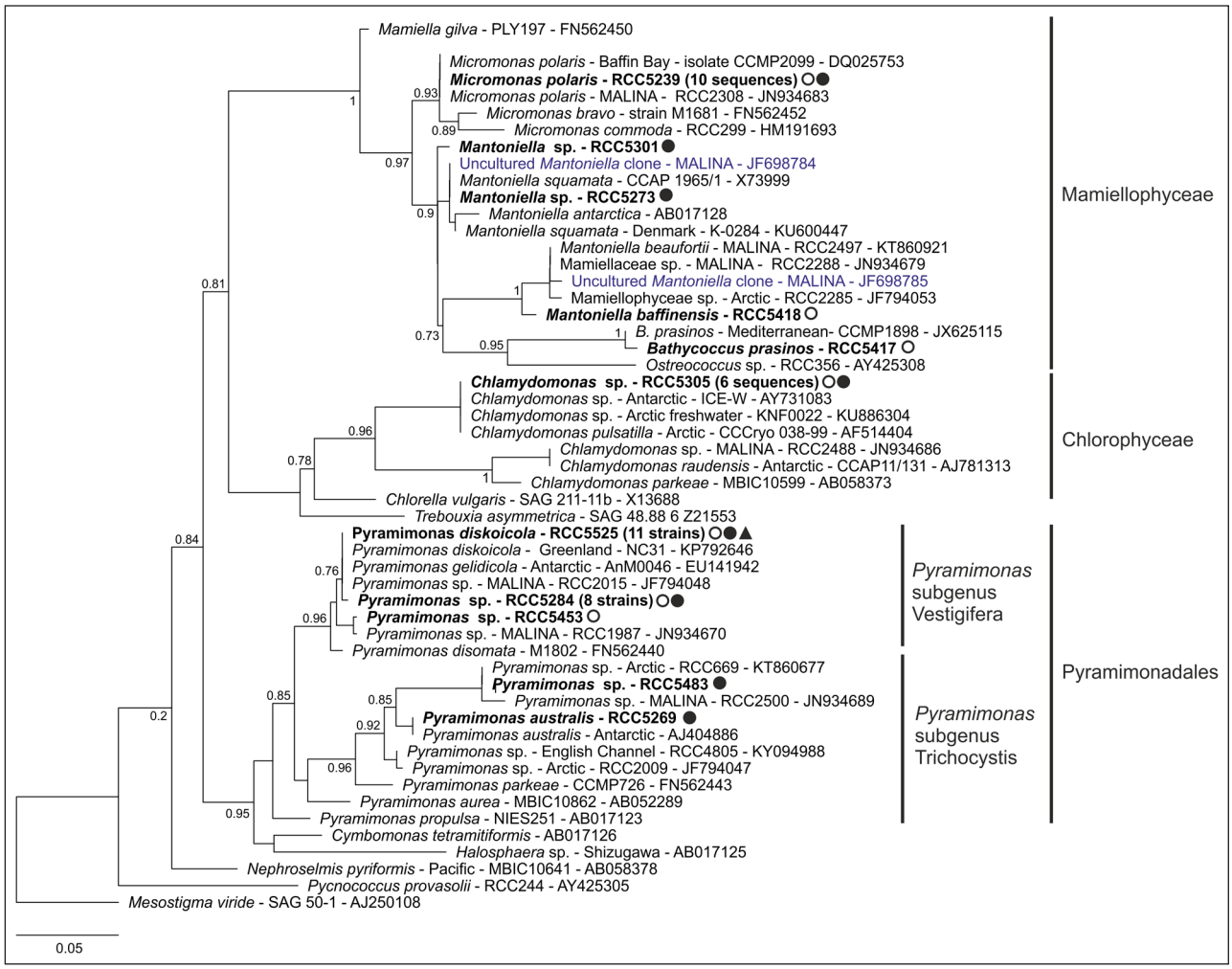

Figure 8: The 18S rRNA phylogenetic tree of Chlorophyta. The 18S rRNA phylogenetic tree inferred by FastTree approximate-maximum-likelihood analysis for the Chlorophyta strains. Legend as in Figure 4, using an alignment of 52 sequences with 361 nucleotide positions. DOI: https://doi.org/10.1525/elementa.401.f8

RCC5525 (**Figure 8**). Cells are pyramidal to round, ~8 μm long with a pyrenoid and basally positioned starch grain, four flagella shorter than cell length, and a flagellar pit ~2 μm deep (**Figure 7G**).

The *Pyramimonas sp.* phylotype represented by **RCC5281** is formed by two IC strains from samples taken at 20-m depth at the peak of the bloom on different sampling days (Supplemntary Data S1). The representative sequence is 100% similar to that of the Arctic strain *Pyramimonas* sp. RCC1987. These strains were lost and no images are available.

Pyramimonas australis **RCC5269** strain from IC water has a sequence matching with 100% similarity that of *P. australis* (GenBank AJ404886) from the subgenus *Trichocystis*, an Antarctic species described based on light/electron microscopy, nuclear-encoded small-subunit ribosomal DNA and chloroplast-encoded *rbc*L gene sequences, but with no representative sequence from cultures until now (Moro et al., 2002). Cells are pear-like to almost oval, ~10 μm long and 6 μm wide with four flagella (**Figure 7E**).

Pyramimonas sp. **RCC5483** strain was recovered from IC surface waters during the pre-bloom phase and its sequence shares 100% similarity with that of the Arctic strain RCC669 (**Figure 8**). This strain was lost and no images are available.

Pyramimonas sp. **RCC5453** was isolated from an IC ice core sample during the pre-bloom phase and its sequence matches with 99.7% similarity that of the Arctic strain *Pyramimonas* sp. RCC1987. Cells are pear-like to round, from 4 to 7 μm long and with four flagella (**Figure 7K**).

Cryptophyta

The *Baffinella frigidus* phylotype represented by **RCC5246** contains 13 strains collected from IC water and ice samples (Supplementary Data S1). Their representative sequence matches with 100% similarity those of the *B. frigidus* sp. strain CCMP2045 (**Figure 6B**). This genus was originally isolated from Baffin Bay and is the first Cryptophyta representative described from this region (Daugbjerg et al., 2018). Cells are ~10 μm long and 5 μm wide with a prominent pyrenoid (**Figure 7A**).

The *Rhodomonas* sp. phylotype represented by **RCC5610** groups 3 strains, 2 of them isolated from IC and one from AM water samples (Supplementary Data S1). Its representative sequence has low similarity to that

of **RCC5246** (96.8%) and is 100% similar to other Arctic strains such as RCC2020 and *Rhodomonas marina* SCCAP K-0435 from Denmark (**Figure 6B**), a species associated with sea ice (Niemi et al., 2011). Cell length is ~18 μm with a ventral to dorsal width ~8 μm, two flagella, and a clearly visible furrow with rows of ejectisomes (**Figure 7R**). This genus is frequently observed in Arctic waters (Lovejoy et al., 2002), being abundant in the subsurface chlorophyll maximum (Joo et al., 2012) or associated with sea ice (Niemi et al., 2011).

Haptophyta

Pseudohaptolina sorokinii strain (**RCC5270**) was retrieved from IC water during the peak of the bloom. Its sequence shares 100% similarity with that of the recently described *P. sorokinii* (Orlova et al., 2016) strain PsAB2015 collected from coastal, under-ice water and 99.7% with the strain *P. arctica* CCMP 1204 (**Figure 6C**). Cells are round to oblong, ~17 μm in length and 12 μm in width. The two flagella have almost the same length as the cell, with a shorter haptonema (**Figure 7F**).

The *Isochrysis* sp. phylotype represented by **RCC5486** contains three strains, all retrieved from IC ice core samples. Their sequence shared low similarity to any other cultured strain in the GenBank database, matching with 99.2% identity the *Isochrysis nuda* strain RCC2477 and 99.1% *Isochrysis galbana* strain 24–25B5 (**Figure 6C**). Cells are solitary, round to oval, ~6 μm long and 5 μm wide. The nucleus, stigma and two 7 μm flagella can be observed (**Figure 7L**). Although mainly isolated from coastal and estuarine environments (Bendif et al., 2013), this genus has also been reported as characteristic of sea-ice environments (Majaneva et al., 2017).

Alveolata (Dinophyta)

The *Biecheleria cincta* phylotype represented by **RCC5518** has three strains, all from AM water samples at 20-m depth during the bloom-development phase (Supplementary Data S1). Sequences from this phylotype are related with 100% identity to the Arctic isolate RCC2013 *Biecheleria cincta* (**Figure 6D**), a cosmopolitan species found also in polar waters (Balzano et al., 2012a), with reported mixotrophic behaviour (Kang et al., 2011). Cells are ~10 μm wide with irregular shaped chloroplasts (**Figure 7O**).

The sequence of *Biecheleria* sp. (**RCC5522**), collected in the same sample as the *B. cincta* **RCC5518** phylotype, differed by only one base pair from the sequence of RCC5518, branching with *B. brevisulcata* strain trd276-kt from freshwater (**Figure 6D**). Cells are spherical to oval, ~8 μm long and 6 μm wide with irregularly shaped chloroplasts (**Figure 7P**).

Culture diversity according to isolation source and method

Ice Camp

A total of 187 strains were isolated from IC samples, 110 from the water and 77 from the ice (Supplementary Data S1). Diatoms dominated isolates from all phases of the bloom (pre-bloom, bloom-development and bloom-peak), although the diversity and number of strains varied (**Figure 9**). During the pre-bloom phase, 28 strains were recovered from the ice and 10 from the water, belonging to six classes (**Figure 9**). This phase was dominated by Bacillariophyceae, mainly *Nitzschia* and *F. cylindrus* (**Figure 9**, Supplementary Data S1). Eight out of the eleven Mediophyceae strains belonged to the genus *Thalassiosira*. Strains from Pyramimonadales, Prymnesiophyceae, Pelagophyceae and Mamiellophyceae were also retrieved during pre-bloom. The bloom-development phase yielded 50 strains from seven classes. New taxa not isolated during the first phase appeared in this second phase, including one strain of Pedinellales (Dictyochophyceae) from an ice sample, and 7 strains of Cryptophyceae assigned to *Rhodomonas* and *Baffinella*, all from water samples (**Figure 9**, Supplementary Data S1). More strains were retrieved during the bloom-peak phase than the other two phases combined (99), and 11 classes were isolated. In contrast to the previous two phases, strains retrieved from water were more diverse than from the ice (**Figure 9**). Chlorophyceae were represented by *Chlamydomonas* sp., from both water and ice samples. One strain of the Prymnesiophyceae *P. sorokinii* and the Chrysophyceae strains *D. faculiferum* and *Spumella* spp. were only retrieved during this phase (Supplementary Data S1). With respect to diatoms, this phase was marked by an increase in Mediophyceae, particularly from the genera *Chaetoceros* and *Attheya* (Supplementary Data S1).

Amundsen cruise

A total of 89 strains were isolated from AM water samples, of which 81 were diatoms. Although some stations were dominated by Bacillariophyceae, such as station G102, the majority of the strains belonged to the Mediophyceae, particularly *Attheya* spp. and *C. neogracilis* (Supplementary Data S1). Only two strains of the Coscinodiscophyceae genus *Actinocyclus* sp. were recovered, both from surface waters at the same station (G713). Few non-diatom strains were isolated. The only station with Cryptophyceae representatives was AM1, from which one *Rhodomonas* strain was isolated (Figure S2). Four Dinophyceae strains (*Biecheleria* spp.) were retrieved from station G204. One strain of *Spumella* sp. was recovered from G110 and two *Pyramimonas* sp. strains from G512 and G707 (Supplementary Data S1).

Isolation method

Serial dilution yielded the most phylotypes (18), followed by FCM cell sorting (14) and single cell pipetting (7). Eighteen phylotypes had representatives isolated by more than one technique (Figure S3). Among diatoms, Bacillariophyceae and Mediophyceae were retrieved by the three isolation methods, but Coscinodiscophyceae were isolated only by single cell pipetting (Figure S4A to C). Specifically, *Arcocellulus* sp. and *E. groenlandica* were retrieved only by flow cytometry sorting, while *B. bathyomphala*, *Coscinodiscus* sp. and *Actinocyclus* sp. strains came only from single cell pipetting. The strains isolated only by serial dilution included *Sellaphora* sp., *Skeletonema* sp. and one Naviculales phylotype (Supplementary Data S1). For non-diatoms,

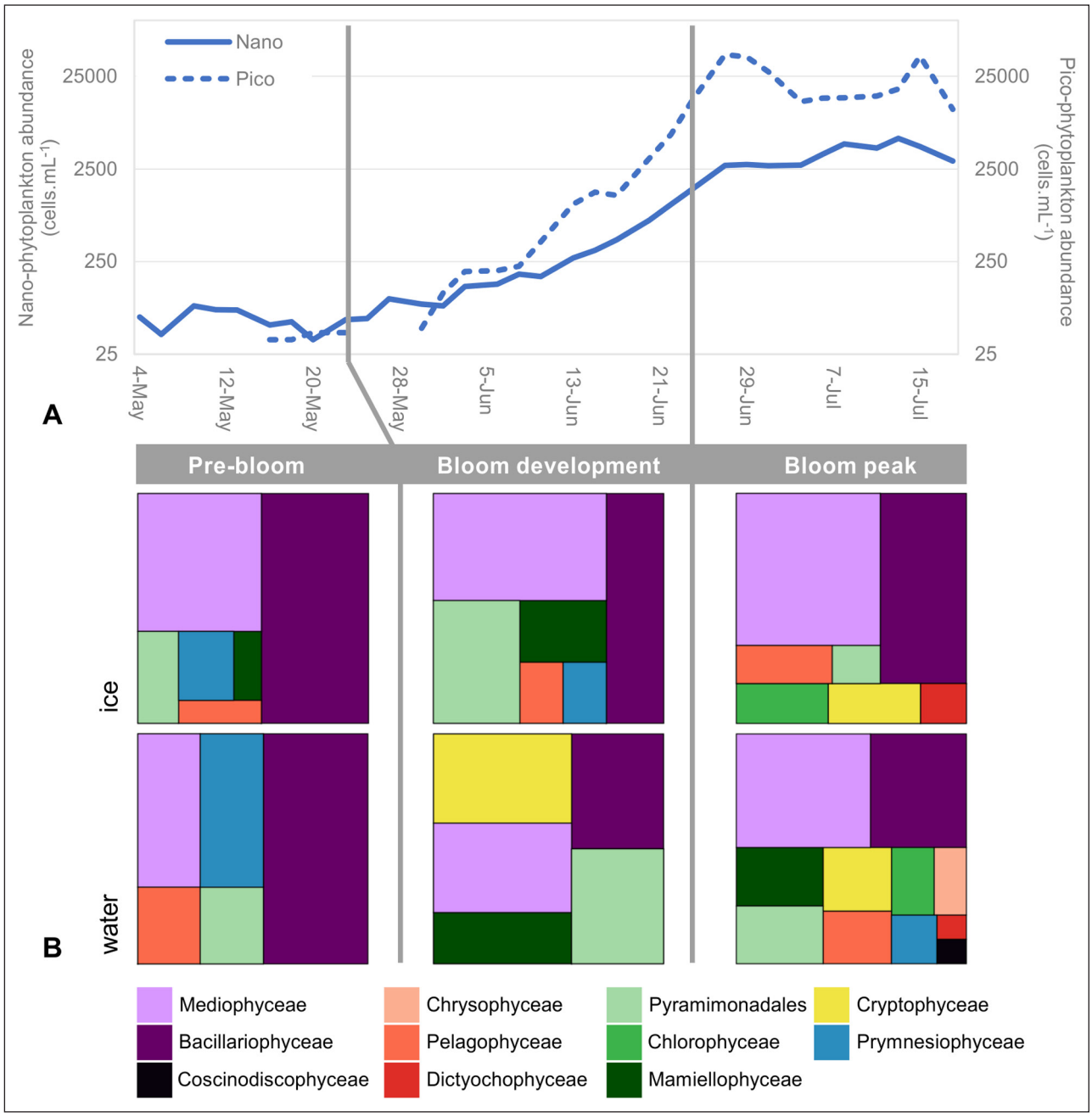

Figure 9: Evolution of culture diversity during the bloom. A) Abundance of pico- (dashed line, right axis) and nano-phytoplankton (solid lines, left axis) measured by flow cytometry at 10-m depth at the Ice Camp location. Phases of the bloom: pre-bloom (May 4 to 23), bloom development (May 24 to June 22) and bloom peak (June 23 to July 18). **B)** Treemaps showing the distribution of strains by class during the different phases of the bloom for the water and sea ice samples. DOI: https://doi.org/10.1525/elementa.401.f9

FCM cell sorting was the technique which retrieved the highest diversity at the class level (Figure S4F). *D. faculiferum*, *Biecheleria* spp., *P. sorokinii*, and two phyloypes of *Mantoniella* sp., were only obtained by this technique. *B. prasinos*, *M. baffinensis* and *Spumella* spp. were recovered only by serial dilution, as well as 9 of 10 *M. polaris* strains.

Discussion

Novel diversity

Half of the strains in this study were retrieved using FCM cell sorting, reflecting previous reports on the efficiency of this isolation technique (Marie et al., 2017). The use of other techniques helped to increase the diversity of taxa successfully cultured, as 68% of phylotypes were obtained by a single isolation method, confirming previous work in the Arctic and other marine systems (Le Gall et al., 2008; Balzano et al., 2012). For instance, although only 12% of strains originated from single cell pipetting, Coscinodiscophyceae were only retrieved by this technique, as well as three of four *Thalassiosira* phylotypes. Serial dilution yielded 38% of the strains and was particularly successful for retrieving picoplanktonic Mamiellophyceae. In fact, at the early stages of isolate characterization (before screening and dereplication), 60 picoplankton strains were

established by this technique, compared to only one by cell sorting and none by single cell pipetting. Among the phylotypes retrieved by more than one isolation method were some well known Arctic taxa such as *A. septentrionalis*, *C. neogracilis* and *F. cylindrus*.

Of the 57 retrieved phylotypes, 32 could not be assigned at the species level and 6, at the genus level. Some species cannot be reliably determined by 18S rRNA sequencing alone, like *T. rotula*, *A. cornucervis* or *C. neogracilis* that may display cryptic diversity. In such cases accurate determination would usually require the use of alternative gene markers such as 28S rRNA or ITS (Balzano et al., 2017), or there may be morphological characters that distinguish the species. For example, the closely related species *A. septentrionalis* and *A. longicornis* cannot be discriminated by 18S rRNA (Rampen et al., 2009), but the latter can be distinguished morphologically by its characteristic long horns.

Of the diversity cultured in this study, pennate diatoms contained the most candidates for novel taxa (i.e., similarity above 99% only to environmental sequences). The five phylotypes affiliated to *Nitzschia* spp. were not closely related to any existing sequenced strain. For example, the *Nitzschia* RCC5458 strain isolated from the ice branched apart from other *Nitzschia* phylotypes with high bootstrap support (95%), with only 98% similarity to a strain from the Red Sea. Also retrieved from the ice, *Cylindrotheca* RCC5303 grouped with *C. closterium* in a moderately supported clade (72%), apparently forming a new lineage within the *C. closterium* species complex (98% similarity). Other pennate diatoms with low sequence identity matches to existing strains included Naviculales sp. RCC5387 and *Sellaphora* sp. RCC5460. With respect to centric diatoms, *Coscinodiscus* RCC5319 had the greatest dissimilarity to any existing strain sequence (95% identity), grouping with moderate bootstrap support (80%) with *C. radiatus* from the North Pacific, a species previously reported from Baffin Bay (Lovejoy et al., 2002). Unfortunately, this strain was lost before morphological analysis was undertaken. *C. decipiens* RCC5606 is interesting in that it is clearly distinguishable from the closely related *C. decipiens* RCC1997 from the Beaufort Sea (99.8% similarity) (Balzano et al., 2017) and differs from the original description (Hasle and Syvertsen, 1997) by its prominently curved chains.

Among green algae, the newly described Arctic species *M. baffinensis* (from RCC5418) and *M. beaufortii* (Yau et al., 2019), as well as the other *Mantoniella*-related strains from this work that were lost (RCC5273 and RCC5301), suggest that this genus is more diverse than other Arctic Mamiellophyceae and hosts several rare species that are not often revealed in environmental sequencing data. The Mamiellophyceae *B. prasinos* (RCC5417) strain that was isolated from ice is, to the best of our knowledge, the only available Arctic isolate of this very ubiquitous species (Tragin and Vaulot, 2019). This will offer interesting perspectives in terms of genome sequencing and physiological experiments, as this strain might correspond to a new cold-adapted ecotype.

The *Isochrysis* sp. strains that originated from sea ice are not closely related to any polar strain or environmental sequence, potentially representing a new cold-adapted phylotype. The retrieval of only one dinoflagellate species, *Biecheleria cincta*, previously *Woloszynskia* (Balzano et al., 2012), is at odds with the known diversity of dinoflagellates in the Arctic (Bachy et al., 2011; Onda et al., 2017) and especially in Baffin Bay (Lovejoy et al., 2002). Another extensive Arctic culture isolation effort yielded a similar result (Balzano et al., 2012), indicating the need for alternative isolation methods to overcome this bias.

Change in diversity during bloom development

The strains recovered were more numerous and more diverse during the bloom itself when sea-ice melted. During the two preliminary phases of the bloom (pre-bloom and bloom-development) the highest strain diversity originated from sea ice samples. A shift occurred as the bloom became established and the water column samples yielded more strain diversity. The number of flagellate strains isolated from water during the bloom increased from 3 during the pre-bloom period to 33 at its peak. Flagellate-dominated communities have been reported in late summer in northern Baffin Bay and the Beaufort Sea (Tremblay et al., 2009). During pre-bloom, flagellates isolated from water samples belonged to only two classes (Pelagophyceae and Pyramimonadales), compared to seven classes during later phases. *Chlamydomonas* (Chlorophyceae), a genus usually associated with freshwater environments, was only isolated in July when ice melting accelerated, lowering the salinity of surface waters. All *Micromonas* and most *Pyramimonas* strains (20 out of 24) were also isolated from the two later phases of the bloom. Both genera have been documented in abundance in lower salinity, summer Arctic waters (Not et al., 2005; Balzano et al., 2012), although higher *M. polaris* abundance has been associated with both pre-bloom and post-bloom stages (Marquardt et al., 2016; Meshram et al., 2017), thriving in both nutrient-replete and nutrient-deplete conditions (Balzano et al., 2012a). Flow cytometry data showed a peak in picoplankton abundance preceding that of nanoplankton (**Figure 9**), a pattern that has been observed previously (Sherr et al., 2003). One *M. polaris* strain was retrieved from an ice core sample during bloom-development, confirming previous studies using high throughput sequencing that have shown that *M. polaris* is part of both Arctic (Comeau et al., 2013) and subarctic sympagic communities (Belevich et al., 2018). *Pyramimonas* cell abundance in the Baffin Bay region during summer is exceptionally high compared to other Arctic domains such as the Bering, Chukchi and Beaufort Seas (Crawford et al., 2018), where it seems to be also fairly diverse (Balzano et al., 2012). Pyramimonadales were indeed the third most represented class in the present study, from both water and ice samples. Ochrophyta strains associated with heterotrophic or mixotrophic behavior such as *Spumella*, *Dinobryon* (Unrein et al., 2010) and Pedinellales (Piwosz and Pernthaler, 2010) were only isolated during the bloom-peak, which might be related to a competitive advantage under nitrogen deprivation in surface waters as the spring bloom develops.

Diatoms play a major role in sympagic assemblages (Mundy et al., 2011), and a pennate dominated community

(Comeau et al., 2013) is considered a mature state of the successional stages during sea ice formation (Niemi et al., 2011; Kauko et al., 2018), when centric diatoms are found in lower numbers (Olsen et al., 2017). *Navicula* and *Nitzschia* representatives thrive in high abundance in the high salinity brine channels (Rózanska et al., 2009; Johnsen et al., 2018). In the present study, eight out of the sixteen phylotypes retrieved solely from ice were pennate diatoms, including two *Navicula* and two *Nitzschia* species. As the ice melts and the bloom develops in the Arctic pelagic environment, bigger cells prosper, including centric diatoms such as *T. nordenskioeldii*, *T. antarctica* var. *borealis* and/or the smaller-sized *C. gelidus* (Booth et al., 2002; Horvat et al., 2017). The relevance of the pelagic environment to centric diatoms was demonstrated by the Bacillariophyceae/Coscinodiscophyceae genera recovered solely from the water column, including *Skeletonema*, *Shionodiscus* and *Actinocyclus*. Although *Thalassiosira* strains were isolated from the first phase of the bloom, including ice samples, *C. gelidus* was only retrieved from mid-June onwards. *C. gelidus* has been often reported in the Arctic (Ardyna et al., 2017; Johnsen et al., 2018), in particular following *Thalassiosira* blooms (Booth et al., 2002). *C. neogracilis* strains alone comprised 12% of all strains and were retrieved from all phases of the bloom, from ice and surface waters down to 35 meters. The wide spatial and temporal range from which this species was retrieved attests for its ubiquity and importance in this environment.

Conclusion

Sea ice, under-ice and open water Arctic phytoplankton communities differ in diversity, biomass, growth rate and tolerance of environmental conditions (Arrigo et al., 2012). Similarly, different types of sea ice provide different substrates, and therefore harbor different communities, as observed between fast, pack and drift ice (Comeau et al., 2013; Majaneva et al., 2017). The same is true for the stages of sea ice formation (Olsen et al., 2017; Kauko et al., 2018). Although many species recovered in this study have been isolated before, ice core samples yielded most of the novel taxa, for all groups from diatoms to green algae. It is important that culturing efforts continue in the Arctic, as ongoing and predicted loss in ice coverage and thickness (Perovich and Richter-Menge, 2009) will certainly impact plankton diversity, dynamics and community structure (Comeau et al., 2011; Blais et al., 2017; Horvat et al., 2017). As the diversity within culture collections improves to reflect the complexity of the environment, the increased amount of validated reference sequences will help scientists to better access eukaryotic plankton distribution patterns across the Arctic. In addition, the availability of polar strains will enable experimental studies to observe physiological and metabolic impacts of current changes such as global warming on polar phytoplankton communities.

Data Accessibility Statement

Strains have been deposited to the Roscoff Culture Collection (http://www.roscoff-culture-collection.org) under numbers RCC5197 to RCC5612 and sequences to Genbank under accession numbers MH764681:765044.

Supplemental file

The supplemental file for this article can be found as follows:

- **Supplementary material.** The supplementary material contains links to two supplementary data files and four supplementary figures. DOI: https://doi.org/10.1525/elementa.401.s1

Acknowledgements

We thank the whole Green Edge team, as well as the *Amundsen* crew, for the help they provided at all stages of this project. Special thanks to Marie-Hélène Forget and Joannie Ferland for the ice camp logistics.

Funding information

Financial support for this work was provided by the Green Edge project (ANR-14-CE01-0017, Fondation Total), the ANR PhytoPol (ANR-15-CE02-0007) and TaxMArc (Research Council of Norway, 268286/E40). M.T. was supported by a PhD fellowship from the Université Pierre et Marie Curie and the Région Bretagne (ARED GreenPhy). ALS was supported by FONDECYT grant PiSCOSouth (N1171802). CGR was supported by CONICYT project 3190827.

Competing interests

The authors have no competing interests to declare.

Author contributions

- Contributed to conception and design: DV, ALS, IP
- Contributed to acquisition of data: CGR, ALS, PG, FLG, DM, MT, IP, DV
- Contributed to analysis and interpretation of data: CGR, ALS, DV
- Drafted and/or revised the article: CGR, ALS, IP, DV
- Approved the submitted version for publication: CGR, ALS, DV, PG, FLG, DM, MT, IP

References

Ardyna, M, Babin, M, Devred, E, Forest, A, Gosselin, M, Raimbault, P and **Tremblay, J-É.** 2017. Shelf-basin gradients shape ecological phytoplankton niches and community composition in the coastal Arctic Ocean (Beaufort Sea). *Limnol Oceanogr* **62**(5): 2113–2132. DOI: https://doi.org/10.1002/lno.10554

Arrigo, KR, Perovich, DK, Pickart, RS, Brown, ZW, van Dijken, GL, Lowry, KE, Mills, MM, Palmer, MA, Balch, WM, Bahr, F, Bates, NR, Benitez-Nelson, C, Bowler, B, Brownlee, E, Ehn, JK, Frey, KE, Garley, R, Laney, SR, Lubelczyk, L, Mathis, J, Matsuoka, A, Mitchell, BG, Moore, GWK, Ortega-Retuerta, E, Pal, S, Polashenski, CM, Reynolds, RA, Schieber, B, Sosik, HM, Stephens, M and **Swift, JH.** 2012. Massive phytoplankton blooms under Arctic sea ice. *Science* **336**(6087): 1408–1408. DOI: https://doi.org/10.1126/science.1215065

Arrigo, KR, Perovich, DK, Pickart, RS, Brown, ZW, van Dijken, GL, Lowry, KE, Mills, MM, Palmer, MA, Balch, WM, Bates, NR, Benitez-Nelson,

CR, Brownlee, E, Frey, KE, Laney, SR, Mathis, J, Matsuoka, A, Greg Mitchell, B, Moore, GWK, Reynolds, RA, Sosik, HM and **Swift, JH.** 2014. Phytoplankton blooms beneath the sea ice in the Chukchi sea. *Deep-Sea Res P II* **105**: 1–16. DOI: https://doi.org/10.1016/j.dsr2.2014.03.018

Arrigo, KR, van Dijken, G and **Pabi, S.** 2008. Impact of a shrinking Arctic ice cover on marine primary production. *Geophys Res Lett* **35**(19): L19603. DOI: https://doi.org/10.1029/2008GL035028

Årthun, M, Eldevik, T, Smedsrud, LH, Skagseth, Ø and **Ingvaldsen, RB.** 2012. Quantifying the influence of Atlantic heat on Barents sea ice variability and retreat. *J Climate* **25**(13): 4736–4743. DOI: https://doi.org/10.1175/JCLI-D-11-00466.1

Assmy, P, Ehn, JK, Fernández-Méndez, M, Hop, H, Katlein, C, Bluhm, K, Daase, M, Engel, A, Fransson, A, Granskog, MA, Stephen, R, Kristiansen, S, Nicolaus, M, Peeken, I, Renner, AHH, Spreen, G, Tatarek, A and **Wiktor, J.** 2013. Floating ice-algal aggregates below melting Arctic sea ice. *PLoS ONE* **8**(10): 1–13. DOI: https://doi.org/10.1371/journal.pone.0076599

Assmy, P, Fernández-Méndez, M, Duarte, P, Meyer, A, Randelhoff, A, Mundy, CJ, Olsen, LM, Kauko, HM, Bailey, A, Chierici, M, Cohen, L, Doulgeris, AP, Ehn, JK, Fransson, A, Gerland, S, Hop, H, Hudson, SR, Hughes, N, Itkin, P, Johnsen, G, King, JA, Koch, BP, Koenig, Z, Kwasniewski, S, Laney, SR, Nicolaus, M, Pavlov, AK, Polashenski, CM, Provost, C, Rösel, A, Sandbu, M, Spreen, G, Smedsrud, LH, Sundfjord, A, Taskjelle, T, Tatarek, A, Wiktor, J, Wagner, PM, Wold, A, Steen, H and **Granskog, MA.** 2017. Leads in Arctic pack ice enable early phytoplankton blooms below snowcovered sea ice. *Sc Reports* **7**: 40850. DOI: https://doi.org/10.1038/srep40850

Bachy, C, Lopez-Garcia, P, Vereshchaka, A and **Moreira, D.** 2011. Diversity and vertical distribution of microbial eukaryotes in the snow, sea ice and seawater near the North Pole at the end of the polar night. *Front Microbiol* **2**: 1–12. DOI: https://doi.org/10.3389/fmicb.2011.00106

Balzano, S, Gourvil, P, Siano, R, Chanoine, M, Marie, D, Lessard, S, Sarno, D and **Vaulot, D.** 2012. Diversity of cultured photosynthetic flagellates in the northeast Pacific and Arctic Oceans in summer. *Biogeosciences* **9**: 4553–4571. DOI: https://doi.org/10.5194/bg-9-4553-2012

Balzano, S, Marie, D, Gourvil, P and **Vaulot, D.** 2012a. Composition of the summer photosynthetic pico and nanoplankton communities in the Beaufort Sea assessed by T-RFLP and sequences of the 18S rRNA gene from flow cytometry sorted samples. *ISME J* **6**: 1480–1498. DOI: https://doi.org/10.1038/ismej.2011.213

Balzano, S, Percopo, I, Siano, R, Gourvil, P, Chanoine, M, Marie, D, Vaulot, D and **Sarno, D.** 2017. Morphological and genetic diversity of Beaufort Sea diatoms with high contributions from the *Chaetoceros neogracilis* species complex. *J Phycol* **53**: 161–187. DOI: https://doi.org/10.1111/jpy.12489

Belevich, TA, Ilyash, LV, Milyutina, IA, Logacheva, MD, Goryunov, DV and **Troitsky, AV.** 2018. Photosynthetic picoeukaryotes in the land-fast ice of the White Sea, Russia. *Microb Ecol* **75**: 582–597. DOI: https://doi.org/10.1007/s00248-017-1076-x

Bendif, EM, Probert, I, Schroeder, DC and **de Vargas, C.** 2013. On the description of *Tisochrysis lutea* gen. nov. sp. nov. and *Isochrysis nuda* sp. nov. in the Isochrysidales, and the transfer of *Dicrateria* to the Prymnesiales (Haptophyta). *J Appl Phycol* **25**: 1763–1776. DOI: https://doi.org/10.1007/s10811-013-0037-0

Blais, M, Ardyna, M, Gosselin, M, Dumont, D, Simon, B, Tremblay, J-E, Gratton, Y, Marchese, C and **Poulin, M.** 2017. Contrasting interannual changes in phytoplankton productivity and community structure in the coastal Canadian Arctic Ocean. *Limnol Oceanogr* **62**: 2480–2497. DOI: https://doi.org/10.1002/lno.10581

Boenigk, J, Pfandl, K, Stadler, P and **Chatzinotas, A.** 2005. High diversity of the '*Spumella*-like' flagellates: an investigation based on the SSU rRNA gene sequences of isolates from habitats located in six different geographic regions. *Environ Microbiol* **7**(5): 685–697. DOI: https://doi.org/10.1111/j.1462-2920.2005.00743.x

Booth, BC, Larouche, P, Bélanger, S, Klein, B, Amiel, D and **Mei, ZP.** 2002. Dynamics of *Chaetoceros socialis* blooms in the North Water. *Deep-Sea Res P II* **49**(22–23): 5003–5025. DOI: https://doi.org/10.1016/S0967-0645(02)00175-3

Brown, ZW and **Arrigo, KR.** 2013. Sea ice impacts on spring bloom dynamics and net primary production in the Eastern Bering Sea. *J Geophys Res: Oceans* **118**(1): 43–62. DOI: https://doi.org/10.1029/2012JC008034

Campbell, K, Mundy, CJ, Belzile, C, Delaforge, A and **Rysgaard, S.** 2017. Seasonal dynamics of algal and bacterial communities in Arctic sea ice under variable snow cover. *Polar Biol* **41**(1): 41–58. DOI: https://doi.org/10.1007/s00300-017-2168-2

Chamnansinp, A, Li, Y, Lundholm, N and **Moestrup, Ø.** 2013. Global diversity of two widespread, colony-forming diatoms of the marine plankton, *Chaetoceros socialis* (syn. *C. radians*) and *Chaetoceros gelidus* sp. nov. *J Phycol* **49**: 1128–1141. DOI: https://doi.org/10.1111/jpy.12121

Cleve, PT. 1896. Diatoms from Baffin Bay and Davis Strait. *Bihang till Kongliga Svenska Vetenskaps-Akademiens Handlingar* **22**: 1–22.

Comeau, AM, Li, WKW, Tremblay, JE, Carmack, EC and **Lovejoy, C.** 2011. Arctic Ocean microbial community structure before and after the 2007 record sea ice minimum. *PLoS ONE* **6**(11): 1–12. DOI: https://doi.org/10.1371/journal.pone.0027492

Comeau, AM, Philippe, B, Thaler, M, Gosselin, M, Poulin, M and **Lovejoy, C.** 2013. Protists in Arctic drift and land-fast sea ice. *J Phycol* **49**(2): 229–240. DOI: https://doi.org/10.1111/jpy.12026

Crawford, DW, Cefarelli, AO, Wrohan, IA, Wyatt, SN and **Varela, DE.** 2018. Spatial patterns in abundance, taxonomic composition and carbon biomass of nano- and microphytoplankton in Subarctic and Arctic Seas. *Prog Oceanogr* **162**(October 2016): 132–159. DOI: https://doi.org/10.1016/j.pocean.2018.01.006

Daugbjerg, N and **Moestrup, Ø.** 1993. Four new species of *Pyramimonas* (Prasinophyceae) from arctic Canada including a light and electron microscopic description of *Pyramimonas quadrifolia* sp. nov. *Eur J Phycol* **28**: 3–16. DOI: https://doi.org/10.1080/09670269300650021

Daugbjerg, N, Norlin, A and **Lovejoy, C.** 2018. *Baffinella frigidus* gen. et sp. nov. (Baffinellaceae fam. nov., Cryptophyceae) from Baffin Bay: Morphology, pigment profile, phylogeny, and growth rate response to three abiotic factors. *J Phycol* **54**(5): 665–680. DOI: https://doi.org/10.1111/jpy.12766

Delmont, TO, Murat, Eren, A, Vineis, JH and **Post, AF.** 2015. Genome reconstructions indicate the partitioning of ecological functions inside a phytoplankton bloom in the Amundsen Sea, Antarctica. *Front Microbiol* **6**: 1–19. DOI: https://doi.org/10.3389/fmicb.2015.01090

Demory, D, Baudoux, AC, Monier, A, Simon, N, Six, C, Ge, P, Rigaut-Jalabert, F, Marie, D, Sciandra, A, Bernard, O and **Rabouille, S.** 2018. Picoeukaryotes of the *Micromonas* genus: sentinels of a warming ocean. *ISME J.* DOI: https://doi.org/10.1038/s41396-018-0248-0

Duerksen, SW, Thiemann, GW and **Budge, SM.** 2014. Large, Omega-3 Rich, pelagic diatoms under Arctic sea ice: sources and implications for food webs. *PloS ONE* **9**(12): 1–18. DOI: https://doi.org/10.1371/journal.pone.0114070

Eilertsen, HC and **Degerlund, M.** 2010. Phytoplankton and light during the northern high-latitude winter. *J Plankton Res* **32**(6): 899–912. DOI: https://doi.org/10.1093/plankt/fbq017

Fernández-Méndez, M, Olsen, LM, Kauko, HM, Meyer, A, Rösel, A, Merkouriadi, I, Mundy, CJ, Ehn, JK, Johansson, AM, Wagner, PM, Ervik, Å, Sorrell, BK and **Duarte, P.** 2018. Algal hot spots in a changing Arctic Ocean: Sea-ice ridges and the snow-ice interface. *Front Mar Sci* **5**: 1–22. DOI: https://doi.org/10.3389/fmars.2018.00075

Grossmann, L, Bock, C, Schweikert, M and **Boenigk, J.** 2015. Small but manifold – hidden diversity in "*Spumella*-like flagellates". *J Euk Microbiol* **0**: 1–21. DOI: https://doi.org/10.1111/jeu.12287

Guillard, RRL and **Hargraves, PE.** 1993. *Stichochrysis immobilis* is a diatom, not a chrysophyte. *Phycologia* **32**(3): 234–236. DOI: https://doi.org/10.2216/i0031-8884-32-3-234.1

Harðardóttir, S, Lundholm, N, Moestrup, Ø and **Nielsen, TG.** 2014. Description of *Pyramimonas diskoicola* sp. nov. and the importance of the flagellate Pyramimonas (Prasinophyceae) in Greenland sea ice during the winter–spring transition. *Polar Biol* **37**(10): 1479–1494. DOI: https://doi.org/10.1007/s00300-014-1538-2

Hasle, GR and **Heimdal, BR.** 1968. Morphology and distribution of the marine centric diatom *Thalassiosira antarctica* Comber. *J Roy Microscop Soc* **88**(3): 357–369. DOI: https://doi.org/10.1111/j.1365-2818.1968.tb00618.x

Hasle, GR, Medlin, LK and **Syvertsen, EE.** 1994. Synedropsis gen. nov., a genus of araphid diatoms associated with sea ice. *Phycologia* **33**(4): 248–270. DOI: https://doi.org/10.2216/i0031-8884-33-4-248.1

Hasle, GR and **Syvertsen, EE.** 1997. Marine diatoms. In: Tomas, CR (ed.), *Identifying Marine Phytoplankton*, 5–385. San Diego, California: Academic Press. ISBN 9780126930184. DOI: https://doi.org/10.1016/B978-012693018-4/50004-5

Horvat, C, Jones, DR, Iams, S, Schroeder, D, Flocco, D and **Feltham, D.** 2017. The frequency and extent of sub-ice phytoplankton blooms in the Arctic Ocean. *Science Adv* **3**: 1–8. DOI: https://doi.org/10.1126/sciadv.1601191

Johnsen, G, Norli, M, Moline, M, Robbins, I, von Quillfeldt, C, Sørensen, K, Cottier, F and **Berge, J.** 2018. The advective origin of an under-ice spring bloom in the Arctic Ocean using multiple observational platforms. *Polar Biol* **41**(6): 1197–1216. DOI: https://doi.org/10.1007/s00300-018-2278-5

Joli, N, Monier, A, Logares, R and **Lovejoy, C.** 2017. Seasonal patterns in Arctic prasinophytes and inferred ecology of *Bathycoccus* unveiled in an Arctic winter metagenome. *ISME J*, 1–14. DOI: https://doi.org/10.1038/ismej.2017.7

Joo, HM, Lee, SH, Jung, SW, Dahms, HU and **Lee, JH.** 2012. Latitudinal variation of phytoplankton communities in the western Arctic Ocean. *Deep-Sea Res P II* **81–84**: 3–17. DOI: https://doi.org/10.1016/j.dsr2.2011.06.004

Kang, NS, Jeong, HJ, Yoo, YD, Yoon, EY, Lee, KH, Lee, K and **Kim, G.** 2011. Mixotrophy in the newly described phototrophic dinoflagellate *Woloszynskia cincta* from western Korean waters: Feeding mechanism, prey species and Effect of prey concentration. *J Euk Microbiol* **58**(2): 152–170. DOI: https://doi.org/10.1111/j.1550-7408.2011.00531.x

Katsuki, K, Takahashi, K, Onodera, J, Jordan, RW and **Suto, I.** 2009. Living diatoms in the vicinity of the North Pole, summer 2004. *Micropaleontology* **55**(2–3): 137–170.

Kauko, HM, Olsen, LM, Duarte, P, Peeken, I, Granskog, MA, Johnsen, G, Fernández-Méndez, M, Pavlov, AK, Mundy, CJ and **Assmy, P.** 2018. Algal colonization of young Arctic sea ice in spring. *Front Mar Sci* **5**: 1–20. DOI: https://doi.org/10.3389/fmars.2018.00199

Kearse, M, Moir, R, Wilson, A, Stones-Havas, S, Cheung, M, Sturrock, S, Buxton, S, Cooper, A, Markowitz, S, Duran, C, Thierer, T, Ashton, B, Meintjes, P and **Drummond, A.** 2012. Geneious Basic: An integrated and extendable desktop software platform for the organization and analysis of

sequence data. *Bioinformatics* **28**(12): 1647–1649. DOI: https://doi.org/10.1093/bioinformatics/bts199

Kilias, ES, Nöthig, EM, Wolf, C and **Metfies, K.** 2014. Picoeukaryote plankton composition off West Spitsbergen at the entrance to the Arctic Ocean. *The J Euk Microbiol*, 1–11. DOI: https://doi.org/10.1111/jeu.12134

Kohlbach, D, Graeve, M, Benjamin, AB, David, C, Peeken, I and **Flores, H.** 2016. The importance of ice algae-produced carbon in the central Arctic Ocean ecosystem: food web relationships revealed by lipid and stable isotope analyses. *Limnol Oceanogr* **61**: 2027–2044. DOI: https://doi.org/10.1002/lno.10351

Larkin, MA, Blackshields, G, Brown, NP, Chenna, R, McGettigan, PA, McWilliam, H, Valentin, F, Wallace, IM, Wilm, A, Lopez, R, Thompson, JD, Gibson, TJ and **Higgins, DG.** 2007. ClustalWand Clustal X version 2.0. *Bioinformatics* **23**(21): 2947–2948. DOI: https://doi.org/10.1093/bioinformatics/btm404

Lee, JM and **Lee, JH.** 2012. Morphological study of the genus *Eucampia* (Bacillariophyceae) in Korean coastal waters. *Algae* **27**(4): 235–247. DOI: https://doi.org/10.4490/algae.2012.27.4.235

Leeuwe, MAV, Tedesco, L, Arrigo, KR, Assmy, P, Meiners, KM, Rintala, J-M, Selz, V, David, N and **Stefels, J.** 2018. Microalgal community structure and primary production in Arctic and Antarctic sea ice: A synthesis. *Elem Sci Anth* **6**(4): 1–25. DOI: https://doi.org/10.1525/elementa.267

Le Gall, F, Rigaut-Jalabert, F, Marie, D, Garczarek, L, Viprey, M, Gobet, A and **Vaulot, D.** 2008. Picoplankton diversity in the South-East Pacific Ocean from cultures. *Biogeosciences* **5**: 203–214. DOI: https://doi.org/10.5194/bg-5-203-2008

Lepère, C, Demura, M, Kawachi, M, Romac, S, Probert, I and **Vaulot, D.** 2011. Whole genome amplification (WGA) of marine photosynthetic eukaryote populations. *FEMS Microbiol Ecol* **76**: 513–523. DOI: https://doi.org/10.1111/j.1574-6941.2011.01072.x

Leu, E, Mundy, CJ, Assmy, P, Campbell, K, Gabrielsen, TM, Gosselin, M, Juul-Pedersen, T and **Gradinger, R.** 2015. Arctic spring awakening – Steering principles behind the phenology of vernal ice algal blooms. *Prog Oceanogr* **139**: 151–170. DOI: https://doi.org/10.1016/j.pocean.2015.07.012

Leu, E, Søreide, JE, Hessen, DO, Falk-Petersen, S and **Berge, J.** 2011. Consequences of changing sea-ice cover for primary and secondary producers in the European Arctic shelf seas: Timing, quantity, and quality. *Prog Oceanogr* **90**: 18–32. DOI: https://doi.org/10.1016/j.pocean.2011.02.004

Li, H, Yang, G, Sun, Y, Wu, S and **Zhang, X.** 2007. *Cylindrotheca closterium* is a species complex as was evidenced by the variations of *rbcL* gene and SSU rDNA. *J Ocean Univ China* **6**(2): 167–174. DOI: https://doi.org/10.1007/s11802-007-0167-6

Li, WK, McLaughlin, FA, Lovejoy, C and **Carmack, EC.** 2009. Smallest algae thrive as the arctic ocean freshens. *Science* **326**: 539. DOI: https://doi.org/10.1126/science.1179798

Lovejoy, C, Legendre, L, Martineau, MJ, Bâcle, J and **Von Quillfeldt, CH.** 2002. Distribution of phytoplankton and other protists in the North Water. *Deep-Sea Res P II* **49**: 5027–5047. DOI: https://doi.org/10.1016/S0967-0645(02)00176-5

Lovejoy, C, Massana, R and **Pedro, C.** 2006. Diversity and distribution of marine microbial eukaryotes in the Arctic Ocean and adjacent seas. *Appl Environ Microbiol* **72**(5): 3085–3095. DOI: https://doi.org/10.1128/AEM.72.5.3085-3095.2006

Lovejoy, C, Vincent, WF, Bonilla, S, Roy, S, Martineau, MJ, Terrado, R, Potvin, M, Massana, R and **Pedrós-Alió, C.** 2007. Distribution, phylogeny, and growth of cold-adapted picoprasinophytes in arctic seas. *J Phycol* **43**(1): 78–89. DOI: https://doi.org/10.1111/j.1529-8817.2006.00310.x

Luddington, IA, Lovejoy, C, Kaczmarska, I and **Moisander, P.** 2016. Species-rich metacommunities of the diatom order Thalassiosirales in the Arctic and northern Atlantic Ocean. *J Plankton Res* **38**(4): 781–797. DOI: https://doi.org/10.1093/plankt/fbw030

Lutz, S, Anesio, AM, Raiswell, R, Edwards, A, Newton, RJ, Gill, F and **Benning, LG.** 2016. The biogeography of red snow microbiomes and their role in melting arctic glaciers. *Nature Comm* **7**: 1–9. DOI: https://doi.org/10.1038/ncomms11968

Majaneva, M, Blomster, J, Müller, S, Autio, R, Majaneva, S, Hyytiäinen, K, Nagai, S and **Rintala, J-M.** 2017. Sea-ice eukaryotes of the Gulf of Finland, Baltic Sea, and evidence for herbivory on weakly shade-adapted ice algae. *Eur J Protistol* **57**: 1–15. DOI: https://doi.org/10.1016/j.ejop.2016.10.005

Malviya, S, Scalco, E, Audic, S, Vincent, F, Veluchamy, A, Bittner, L, Poulain, J, Wincker, P, Iudicone, D, de Vargas, C, Zingone, A and **Bowler, C.** 2016. Insights into global diatom distribution and diversity in the world's ocean. *Proc Nat Acad Sci USA* **348**(6237): 1–10. DOI: https://doi.org/10.1073/pnas.1509523113

Marie, D, Le Gall, F, Edern, R, Gourvil, P and **Vaulot, D.** 2017. Improvement of phytoplankton culture isolation using single cell sorting by flow cytometry. *J Phycol* **53**(2): 271–282. DOI: https://doi.org/10.1111/jpy.12495

Marquardt, M, Vader, A, Stübner, EI, Reigstad, M and **Gabrielsen, TM.** 2016. Strong seasonality of marine microbial eukaryotes in a high-Arctic fjord (Isfjorden, in West Spitsbergen, Norway). *Appl Environ Microbiol* **82**(6): 1868–1880. DOI: https://doi.org/10.1128/AEM.03208-15

Massicotte, P, Amiraux, R, Amyot, MP, Archambault, P, Ardyna, M, Arnaud, L, Artigue, L, Aubry, C, Ayotte, P, Bécu, G, Bélanger, S, Benner, R, Bittig, HC, Bricaud, A, Brossier, É, Bruyant, F, Chauvaud, L, Christiansen-Stowe, D, Claustre, H, Cornet-Barthaux, V, Coupel, P, Cox, C, Delaforge, A, Dezutter, T, Dimier, C, Dominé, F, Dufour, F, Dufresne, C, Dumont, D, Ehn, J, Else, B, Ferland, J, Forget, MH, Fortier, L, Galí, M, Galindo, V,

Gallinari, M, Garcia, N, Gérikas-Ribeiro, C, Gourdal, M, Gourvil, P, Goyens, C, Grondin, PL, Guillot, P, Guilmette, C, Houssais, MN, Joux, F, Lacour, L, Lacour, T, Lafond, A, Lagunas, J, Lalande, C, Laliberté, J, Lambert-Girard, S, Larivière, J, Lavaud, J, Le Gall, F, LeBaron, A, Leblanc, K, Legras, J, Lemire, M, Levasseur, M, Leymarie, E, Leynaert, A, dos Santos, A, Lourenço, A, Mah, D, Marec, C, Marie, D, Martin, N, Marty, C, Marty, S, Massé, G, Matsuoka, A, Matthes, L, Moriceau, B, Muller, PE, Mundy, CJ, Neukermans, G, Oziel, L, Panagiotopoulos, C, Pangazi, JJ, Picard, G, Picheral, M, du Sel, F, Pogorzelec, N, Probert, I, Queguiner, B, Raimbault, P, Ras, J, Rehm, E, Reimer, E, Rontani, JF, Rysgaard, S, Saint-Béat, B, Sampei, M, Sansoulet, J, Schmidt, S, Sempéré, R, Sévigny, C, Shen, Y, Tragin, M, Tremblay, JÉ, Vaulot, D, Verin, G, Vivier, F, Vladoiu, A, Whitehead, J and **Babin, M.** 2020. Green Edge ice camp campaigns: understanding the processes controlling the under-ice Arctic phytoplankton spring bloom. *Earth Syst Sci Data* **12**: 151–176. DOI: https://doi.org/10.5194/essd-12-151-2020

Meshram, AR, Vader, A, Kristiansen, S and **Gabrielsen, TM.** 2017. Microbial eukaryotes in an Arctic under-ice spring bloom North of Svalbard. *Front Microbiol* **8**: 1–12. DOI: https://doi.org/10.3389/fmicb.2017.01099

Mock, T, Robert, P, Strauss, J, Mcmullan, M, Paajanen, P, Schmutz, J, Salamov, A, Sanges, R, Toseland, A, Ward, BJ, Allen, AE, Dupont, CL, Frickenhaus, S, Falciatore, A, Ferrante, MI, Gruber, A, Hipkin, R, Janech, MG, Kroth, PG, Fortunato, AE, Glöckner, G, Leese, F, Lindquist, EA, Lyon, BR, Martin, J, Mayer, C, Parker, M, Quesneville, H, Raymond, JA, Uhlig, C, Valas, RE, Valentin, KU, Worden, AZ and **Armbrust, EV.** 2017. Evolutionary genomics of the cold-adapted diatom *Fragilariopsis cylindrus*. *Nature* **541**: 536–540. DOI: https://doi.org/10.1038/nature20803

Moro, I, Rocca, NL, Valle, LD, Moschin, E, Negrisolo, E and **Andreoli, C.** 2002. *Pyramimonas australis* sp. nov. (Prasinophyceae, Chlorophyta) from Antarctica: fine structure and molecular phylogeny. *Eur J Phycol* **37**: 103–114. DOI: https://doi.org/10.1017/S0967026201003493

Mundy, CJ, Gosselin, M, Ehn, JK, Belzile, C, Poulin, M, Alou, E, Roy, S, Hop, H, Lessard, S, Papakyriakou, TN, Barber, DG and **Stewart, J.** 2011. Characteristics of two distinct high-light acclimated algal communities during advanced stages of sea ice melt. *Polar Biol* **34**(12): 1869–1886. DOI: https://doi.org/10.1007/s00300-011-0998-x

Neukermans, G, Oziel, L and **Babin, M.** 2018. Increased intrusion of warming Atlantic waters leads to rapid expansion of temperate phytoplankton in the Arctic. *Glob Change Biol*, 1–9. DOI: https://doi.org/10.1111/gcb.14075

Niemi, A, Michel, C, Hille, K and **Poulin, M.** 2011. Protist assemblages in winter sea ice: setting the stage for the spring ice algal bloom. *Polar Biol* **34**: 1803–1817. DOI: https://doi.org/10.1007/s00300-011-1059-1

Not, F, Massana, R, Latasa, M, Marie, D, Colson, C, Eikrem, W, Pedrós-Alió, C, Vaulot, D and **Simon, N.** 2005. Late summer community composition and abundance of photosynthetic picoeukaryotes in Norwegian and Barents Seas. *Limnol Oceanogr* **50**(5): 1677–1686. DOI: https://doi.org/10.4319/lo.2005.50.5.1677

Olsen, LM, Laney, SR, Duarte, P, Kauko, HM, Fernández-méndez, M, Mundy, CJ, Rösel, A, Meyer, A, Itkin, P, Cohen, L, Peeken, I, Tatarek, A, Różańska-Pluta, M, Wiktor, J, Taskjelle, T, Pavlov, AK, Hudson, SR, Granskog, MA, Hop, H and **Assmy, P.** 2017. The multiyear ice seed repository hypothesis. *J Geophys Res: Biogeosciences* **122**: 1529–1548. DOI: https://doi.org/10.1002/2016JG003668

Onda, DFL, Medrinal, E, Comeau, AM, Thaler, M, Babin, M and **Lovejoy, C.** 2017. Seasonal and interannual changes in ciliate and dinoflagellate species assemblages in the Arctic Ocean (Amundsen Gulf, Beaufort Sea, Canada). *Front Mar Sci* **4**(January). DOI: https://doi.org/10.3389/fmars.2017.00016

Orlova, TY, Efimova, KV and **Stonik, IV.** 2016. Morphology and molecular phylogeny of *Pseudohaptolina sorokinii* sp. nov. (Prymnesiales, Haptophyta) from the Sea of Japan, Russia. *Phycologia* **55**(5): 506–514. DOI: https://doi.org/10.2216/15-107.1

Percopo, I, Ruggiero, M, Balzano, S, Gourvil, P, Lundhölm, N, Siano, R, Tammilehto, A, Vaulot, D and **Sarno, D.** 2016. *P. arctica* sp. nov., a new cold-water cryptic *Pseudo-nitzschia* species within the *P. pseudodelicatissima* complex. *J Phycol* **52**: 184–199. DOI: https://doi.org/10.1111/jpy.12395

Perovich, DK and **Richter-Menge, JA.** 2009. Loss of sea ice in the Arctic. *Annu Rev Mar Sci* **1**(1): 417–441. DOI: https://doi.org/10.1146/annurev.marine.010908.163805

Perrette, M, Yool, A, Quartly, GD and **Popova, EE.** 2011. Near-ubiquity of ice edge blooms in the Arctic. *Biogeosciences* **8**: 515–524. DOI: https://doi.org/10.5194/bg-8-515-2011

Piwosz, K and **Pernthaler, J.** 2010. Seasonal population dynamics and trophic role of planktonic nanoflagellates in coastal surface waters of the Southern Baltic Sea. *Environ Microbiol* **12**(2): 364–377. DOI: https://doi.org/10.1111/j.1462-2920.2009.02074.x

Pocock, T, Lachance, MA, Proschold, T, Priscu, JC, Kim, SS and **Huner, NPA.** 2004. Identification of a psychrophilic green alga from Lake Bonney Antarctica: *Chlamydomonas raudensis* ettl. (UWO 241) Chlorophyceae. *J Phycol* **40**: 1138–1148. DOI: https://doi.org/10.1111/j.1529-8817.2004.04060.x

Potvin, M and **Lovejoy, C.** 2009. PCR-based diversity estimates of artificial and environmental 18S rRNA gene libraries. *J Euk Microbiol* **56**(2): 174–181. DOI: https://doi.org/10.1111/j.1550-7408.2008.00386.x

Poulíčková, A, Špačková, J, Kelly, MG, Duchoslav, M and **Mann, DG.** 2008. Ecological variation within *Sellaphora* species complexes (Bacillariophyceae):

Specialists or generalists? *Hydrobiologia* **614**(1): 373–386. DOI: https://doi.org/10.1007/s10750-008-9521-y

Poulin, M, Daugbjerg, N, Gradinger, R, Ilyash, L, Ratkova, T and **von Quillfeldt, C.** 2011. The pan-Arctic biodiversity of marine pelagic and sea-ice unicellular eukaryotes: A first-attempt assessment. *Mar Biodiversity* **41**(1): 13–28. DOI: https://doi.org/10.1007/s12526-010-0058-8

Price, MN, Dehal, PS and **Arkin, AP.** 2010. FastTree 2 – approximately maximumlikelihood trees for large alignments. *PLoS ONE* **5**(3): e9490. DOI: https://doi.org/10.1371/journal.pone.0009490

Quillfeldt, CHV. 2000. Common diatom species in Arctic spring blooms: Their distribution and abundance. *Botanica Marina* **43**: 499–516. DOI: https://doi.org/10.1515/BOT.2000.050

Quillfeldt, CHV. 2004. The diatom *Fragilariopsis cylindrus* and its potential as an indicator species for cold water rather than for sea ice. *Vie et Milieu* **54**(2–3): 137–143.

Rampen, SW, Schouten, S, Elda Panoto, F, Brink, M, Andersen, RA, Muyzer, G, Abbas, B and **Sinninghe Damsté, JS.** 2009. Phylogenetic position of *Attheya longicornis* and *Attheya septentrionalis* (Bacillariophyta). *J Phycol* **45**(2): 444–453. DOI: https://doi.org/10.1111/j.1529-8817.2009.00657.x

Rippka, R, Coursin, T, Hess, W, Lichtle, C, Scanlan, DJ, Palinska, KA, Iteman, I, Partensky, F, Houmard, J and **Herdman, M.** 2000. *Prochlorococcus marinus* Chisholm et al. 1992 subsp. *pastoris* subsp. nov. strain PCC 9511, the first axenic chlorophyll *a2/b2*–containing cyanobacterium (Oxyphotobacteria). *Int J Syst Evol Microbiol* **50**: 1833–1847. DOI: https://doi.org/10.1099/00207713-50-5-1833

Rózanska, M, Gosselin, M, Poulin, M, Wiktor, JM and **Michel, C.** 2009. Influence of environmental factors on the development of bottom ice protist communities during the winter – spring transition. *Mar Ecol Progr Ser* **386**: 43–59. DOI: https://doi.org/10.3354/meps08092

Schmidt, K, Brown, T, Belt, S, Ireland, L, Taylor, KWR, Thorpe, S, Ward, P and **Atkinson, A.** 2018. Do pelagic grazers benefit from sea ice? Insights from the Antarctic sea ice proxy IPSO25. *Biogeosciences* **15**: 1987–2006. DOI: https://doi.org/10.5194/bg-15-1987-2018

Sherr, EB, Sherr, BF, Wheeler, PA and **Thompson, K.** 2003. Temporal and spatial variation in stocks of autotrophic and heterotrophic microbes in the upper water column of the central Arctic Ocean. *Deep-Sea Res P I* **50**(5): 557–571. DOI: https://doi.org/10.1016/S0967-0637(03)00031-1

Simmons, MP, Bachy, C, Sudek, S, Van Baren, MJ, Sudek, L, Ares, M and **Worden, AZ.** 2015. Intron invasions trace algal speciation and reveal nearly identical arctic and Antarctic *Micromonas* populations. *Molec Biol Evol* **32**(9): 2219–2235. DOI: https://doi.org/10.1093/molbev/msv122

Simon, N, Foulon, E, Grulois, D, Six, C, Desdevises, Y, Latimier, M, Le Gall, F, Tragin, M, Houdan, A, Derelle, E, Jouenne, F, Marie, D, Le Panse, S, Vaulot, D and **Marin, B.** 2017. Revision of the genus *Micromonas* Manton et Parke (Chlorophyta, Mamiellophyceae), of the type species *M. pusilla* (Butcher) Manton & Parke and of the species *M. commoda* van Baren, Bachy and Worden and description of two new species based on the genetic and phenotypic characterization of cultured isolates. *Protist* **168**(5): 612–635. DOI: https://doi.org/10.1016/j.protis.2017.09.002

Terrado, R, Scarcella, K, Thaler, M, Vincent, WF and **Lovejoy, C.** 2013. Small phytoplankton in Arctic seas: Vulnerability to climate change. *Biodiversity* **14**(1): 2–18. DOI: https://doi.org/10.1080/14888386.2012.704839

Tragin, M and **Vaulot, D.** 2019. Novel diversity within marine Mamiellophyceae (Chlorophyta) unveiled by metabarcoding. *Sci Reports* **9**(1): 5190. DOI: https://doi.org/10.1038/s41598-019-41680-6

Tremblay, G, Belzile, C, Gosselin, M, Poulin, M, Roy, S and **Tremblay, JÉ.** 2009. Late summer phytoplankton distribution along a 3500 km transect in Canadian Arctic waters: Strong numerical dominance by picoeukaryotes. *Aquat Microb Ecol* **54**(1): 55–70. DOI: https://doi.org/10.3354/ame01257

Unrein, F, Gasol, JM and **Massana, R.** 2010. *Dinobryon faculiferum* (Chrysophyta) in coastal Mediterranean seawater: Presence and grazing impact on bacteria. *J Plankton Res* **32**(4): 559–564. DOI: https://doi.org/10.1093/plankt/fbp150

Vincent, WF. 2010. Microbial ecosystem responses to rapid climate change in the Arctic. *ISME J* **4**(9): 1089–1091. DOI: https://doi.org/10.1038/ismej.2010.108

Whittaker, KA, Rignanese, DR, Olson, RJ and **Rynearson, TA.** 2012. Molecular subdivision of the marine diatom *Thalassiosira rotula* in relation to geographic distribution, genome size, and physiology. *BMC Evol Biol* **12**(209): 2–14. DOI: https://doi.org/10.1186/1471-2148-12-209

Worden, AZ, Lee, JH, Mock, T, Rouzé, P, Simmons, MP, Aerts, AL, Allen, AE, Cuvelier, ML, Derelle, E, Everett, MV, Foulon, E, Grimwood, J, Gundlach, H, Henrissat, B, Napoli, C, McDonald, SM, Parker, MS, Rombauts, S, Salamov, A, Von Dassow, P, Badger, JH, Coutinho, PM, Demir, E, Dubchak, I, Gentemann, C, Eikrem, W, Gready, JE, John, U, Lanier, W, Lindquist, EA, Lucas, S, Mayer, KFX, Moreau, H, Not, F, Otillar, R, Panaud, O, Pangilinan, J, Paulsen, I, Piegu, B, Poliakov, A, Robbens, S, Schmutz, J, Toulza, E, Wyss, T, Zelensky, A, Zhou, K, Armbrust, EV, Bhattacharya, D, Goodenough, UW, Van de Peer, Y and **Grigoriev, IV.** 2009. Green evolution and dynamic adaptations revealed by genomes of the marine picoeukaryotes *Micromonas*. *Science*

324: 268–272. DOI: https://doi.org/10.1126/science.1167222

Yau, S, Lopes dos Santos, A, Eikrem, W, Gérikas Ribeiro, C, Gourvil, P, Balzano, S, Escande, M-L, Moreau, H and **Vaulot, D.** 2019. *Mantoniella beaufortii* and *Mantoniella baffinensis* sp. nov. (Mamiellales, Mamiellophyceae), two new green algal species from the high Arctic. *J Phycol*. In press. DOI: https://doi.org/10.1111/jpy.12932

Zhu, F, Massana, R, Not, F, Marie, D and **Vaulot, D.** 2005. Mapping of picoeucaryotes in marine ecosystems with quantitative PCR of the 18S rRNA gene. *FEMS Microbiol Ecol* **52**: 79–92. DOI: https://doi.org/10.1016/j.femsec.2004.10.006

How to cite this article: Gérikas Ribeiro, C, dos Santos, AL, Gourvil, P, Le Gall, F, Marie, D, Tragin, M, Probert, I and Vaulot, D. 2020. Culturable diversity of Arctic phytoplankton during pack ice melting. *Elem Sci Anth,* 8: 6. DOI: https://doi.org/10.1525/elementa.401

Domain Editor-in-Chief: Jody W. Deming, School of Oceanography, University of Washington, US

Associate Editor: Christine Michel, Fisheries and Oceans Canada, Freshwater Institute, CA

Knowledge Domain: Ocean Science

Part of an *Elementa* Special Feature: Green Edge

Submitted: 13 May 2019 **Accepted:** 30 December 2019 **Published:** 14 February 2020

ELEMENTA Science of the Anthropocene

Elem Sci Anth is a peer-reviewed open access journal published by University of California Press.

OPEN ACCESS